Informes Técnicos Ciemat

1511

OCTUBRE, 2022

ANALYSIS OF THE COLLOIDAL PROPERTIES OF DIFFERENT CLAY MINERALS: IMPACT ON BARRIER PERFORMANCE

Missana, T.
Alonso de los Ríos, U.
Fernández Díaz, A. M.

GOBIERNO DE ESPAÑA
MINISTERIO DE CIENCIA E INNOVACIÓN

Ciemat
Centro de Investigaciones Energéticas, Medioambientales y Tecnológicas

Publication available in catalog of official publications

ISSN: 2695-8864
NIPO: 832-22-007-5

Edition and Publication:
Editorial CIEMAT
Avda. Complutense, 40 28040-MADRID
e-mail: editorial@ciemat.es
Editorial news

ANALISIS DE LAS PROPIEDADES COLOIDALES DE DIFERENTES ARCILLAS: IMPACTO EN LA EFICIENCIA DE BARRERAS

Missana, T.; Alonso de los Ríos, U.; Fernández Díaz, A. M.

72 pp, 31 figs., 10 tbls., 110 ref.

Resumen:

Este estudio analiza el comportamiento coloidal de diferentes bentonitas que se emplean como barrera de ingeniería en los almacenamientos geológicos profundos (AGP) de residuos radioactivos de alta actividad. La erosión de la bentonita y la formación de partículas coloidales comprometerían la seguridad del AGP: la pérdida de masa afectaría el rendimiento del sistema y los coloides de arcilla podrían contribuir al transporte de los radionucleidos.

Las principales características de los coloides generados por diferentes esmectitas (como mineral mayoritario en las bentonitas), -masa de partículas coloidales, tamaño de partícula y carga eléctrica superficial-, se relacionan con las propiedades fisicoquímicas intrínsecas de las arcilla: cationes intercambiables, carga eléctrica total y su distribución entre la capa tetraédrica y octaédrica. Como objetivo final, se compara la formación de coloides con la erosión que experimentan las arcillas en condiciones compactadas y confinadas, simulando las condiciones de un AGP.

ANALYSIS OF THE COLLOIDAL PROPERTIES OF DIFFERENT CLAY MINERALS: IMPACT ON BARRIER PERFORMANCE

Missana, T.; Alonso de los Ríos, U.; Fernández Díaz, A. M.

72 pp, 31 figs., 10 tbls., 110 ref.

Abstract:

This study analysed the characteristics of colloids generated from different smectites, used as engineered barriers in high-level radioactive waste (HLRW) repositories. The erosion of the bentonite would pose a potential problem, because a significant mass loss may jeopardize the performance of the material; furthermore, clay colloids released from the eroded material may play a role on radionuclide transport.

The main characteristics of the colloids generated by different smectites (as the main mineral in bentonites), -mass of colloidal particles, particle size and surface electrical charge-, are related to the intrinsic physicochemical properties of the clay: exchangeable cations, total electrical charge and its distribution between the tetrahedral and octahedral layer.

As final aim, the colloids amounts measured in dispersed experiments were compared to the erosion experienced by the same bentonites in compacted and confined conditions, simulating the conditions present in HLRW repository.

ACKNOWLEDGEMENTS

The compilation of this document was supported by the Innovation Programme under Grant Agreement no. 847593 (EURAD, CORI) and by the Spanish Ministry of Science Innovation (PID2019–106398GB-I00, ARNO Project). The personnel of the Division of Chemistry of CIEMAT is acknowledged for their support in chemical analyses.

INDEX

LIST OF FIGURES

LIST OF TABLES

1 INTRODUCTION

1.1 MOTIVATION

Smectite clay minerals, and their suspensions, are of great scientific interest for their wide range of industrial and environmental fields of application, as nanocomposite, drilling fluids, adsorbents, paints, and for the confinement of hazardous waste [1,2]. In the last century, since the decade of '70, their physicochemical attributes have been studied in detail to establish their adequacy for different uses.

Bentonites, being clay materials with high smectite content, have been largely investigated for their use as barrier and buffer materials in high-level radioactive waste (HLRW) deep geological repositories (DGR) [3]. DGR are the most accepted option for the final storage of high-level radioactive waste [4], and consists on a multibarrier system emplaced hundred meters depth in a geological formation. Crystalline rock and sedimentary clays are the most adequate host rocks. Between the waste and the host different engineered barriers, as metal canisters and compacted bentonites are interposed to hinder radionuclides (RN) migration until their radioactivity has decayed below harmful levels.

Compacted bentonite is a suitable material for engineered barriers in radioactive waste repository for its low permeability, low hydraulic conductivity, for their swelling capacity, plasticity, ability to seal cracks and high sorption capacity, amongst other very interesting properties [3, 5,6,7,8,9].

Despite its expected protective behaviour, to guarantee the long-term safety of a DGR, performance assessment studies demand the thorough analysis of any mechanism that may affect the integrity of the barriers, and therefore compromise safety. The possible erosion of the bentonite barrier of a HLRW repository, leading to the generation of bentonite colloids, is an issue of great concern [10]. A significant bentonite mass loss would compromise the functionality and integrity of the barrier at the long term and because, the eroded particles of colloidal nature, might contribute to radionuclide migration if favourable environmental conditions exist [2,11,12,13].

These undesirable phenomena demand robust theoretical models capable to calculate the possible extent of bentonite eroded mass [14,15] and to predict colloid-mediated radionuclide migration [16], under different environmental conditions. New experimental data are still required to develop them.

In a repository, the arrival of groundwater through the host rock will promote clay barrier hydration and, after its hydration and swelling, the bentonite will penetrate fractures. When groundwater touches the clay, the removal of particles can be produced either by diffusion in water or by mechanical forces. Clay erosion could be promoted by mechanical stresses produced by the water flowing at its surface, which would also facilitate the dragging of particles and aggregates. This mechanical erosion is expected to depend on water velocity and fracture characteristics [10,17,18,19].

Nevertheless, the chemistry of the system is extremely important on clay erosion processes and might be a dominant factor even in the presence of a water flow, as it has been reported elsewhere [11, 12, 20]. The probability of clay erosion increases, in fact, with its capacity to spontaneously disperse in water [21]. Thus, the release of particles from the gel is governed by the colloidal properties of the clay and by those factors that cause dispersion or flocculation which are dependent on the chemistry of the system.

The potential relevance of the intrinsic physicochemical characteristics of smectites on erosion processes has not been analysed in detail so far. In this study, different natural smectites, or bentonites with high smectite content, were selected to understand the main properties (i.e., composition of the interlayer cations, clay layer charge and charge distribution between the tetrahedral and octahedral layer) affecting their colloidal behaviour and potentially favouring/hindering colloid detachment from the bulk (erosion). Furthermore, as the main colloidal properties (size and surface charge) also control many important processes as migration, filtration, sedimentation, interaction with rocks and contaminants, they were determined and related to the abovementioned physicochemical properties. The stability of clay colloids against changes in aqueous ion concentration (Na, Ca) was also analysed.

Clays were selected trying to cover a range of possibilities in terms of main exchangeable cation, layer charge, charge distribution etc. Colloids were extracted suspending the clays in deionized water, to maximize their dispersion, and collecting the supernatant after centrifuging and their characteristics analysed in depth.

The results will be discussed in a generalised form, comparing the free-dispersion results with other experiments in which the erosion of same clays was analysed under compacted and confined conditions [22]. The potential erodibility of different smectites and the implications of this process on the overall performance of the bentonite barrier of a HLWR.

1.2 SMECTITE STRUCTURE AND PROPERTIES

Smectite clays are 2:1 layer phyllosilicates where two (silica) tetrahedral, T, sheets sandwich an octahedral, O, sheet forming a TOT structure, or a clay mineral layer (Figure 1) [2, 23].

Each tetrahedron consists of a cation (Si^{4+}, Al^{3+}, Fe^{3+}) coordinated to four oxygen atoms ($M_{tet}O_4$) and linked to adjacent tetrahedra by sharing three corners forming an infinite two-dimensional hexagonal mesh pattern along the a, b crystallographic directions.

In each octahedron, a cation is framed by O_2- or OH- anions ($M_{oct}O_6$): four apical oxygens of the two adjacent tetrahedral sheets and two OH- radicals. Connections between each octahedron (M) to neighbouring octahedra are made by sharing edges, forming sheets of hexagonal or pseudo-hexagonal symmetry. Octahedra show two different topologies related to the OH- position: cis- or M_2 sites (OH- groups located on opposite corners of the octahedron) and trans-orientation or M_1 sites (OH- atoms located on the same edge of the octahedron).

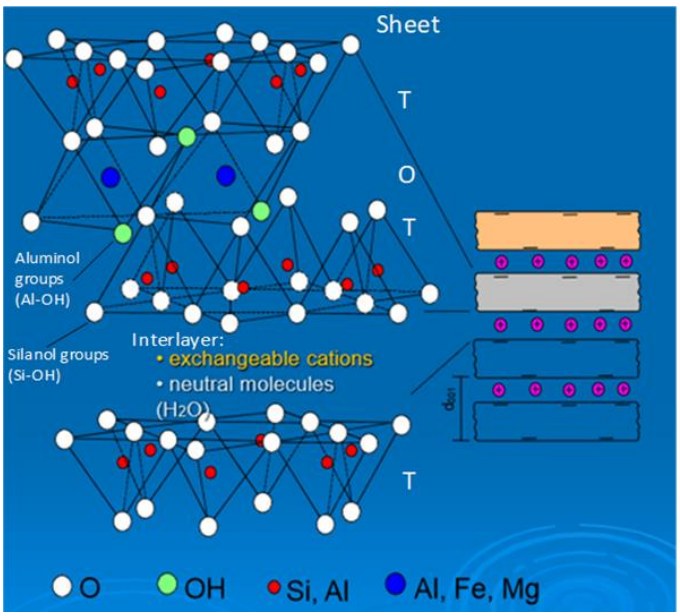

Figure 1. Schematic of the smectite clay structure

In a 2:1 layer structure, the unit cell includes six octahedral sites (four cis- and two trans-oriented) and eight tetrahedral sites. The structural formula is often reported based on the half unit-cell content, i.e., it is based on three octahedral sites (two cis- or M_2 oriented and one trans- or M_1 oriented).

The M_{oct} cations in the octahedral sheet may be either: (a) divalent cations (Mg^{2+}, Fe^{2+}), which occupy all the six octahedral sites. In this case clay mineral is know as tri-octahedral (Tri-), with a structure similar to a brucite-like tri-octahedral sheet [$Mg_3(OH)_6$]. (b) trivalent cations (Al^{3+}, Fe^{3+}) which occupy only four of the six octahedra (M_2 sites), i.e., only two-thirds of the octahedral sites are occupied, one-third being vacant. The clay mineral is known as di-octahedral (Di-), with a structure similar to a gibbsite-like di-octahedral sheet [$Al_2(OH)_6$].

In a di-octahedral smectite, the position of the OH- groups in a vacant octahedral site is configured at cis-vacant (C2 symmetry) or trans-vacant (C2/m symmetry) position.

The general formula (per half unit cell) for di-octahedral smectites is presented in equation (1):

$$(Si_{4-x}\,Al_x)\,(R^{3+}{}_{2-y}R^{2+}{}_y)(M^{+}{}_{x+y}\cdot nH_2O)O_{10}(OH)_2 \qquad (1)$$

and that for trioctahedral clays is shown in equation (2):

$$(Si_{4-x}\,Al_x)\,(R^{2+}{}_{3-y}R^{3+}{}_y)(M^{+}{}_{x+y}\cdot nH_2O)O_{10}(OH)_2 \qquad (2)$$

where, x and y indicate the layer charge resulting from substitutions in tetrahedral and octahedral sites, respectively; R^{2+} and R^{3+} refer to a generic divalent and trivalent octahedral cation, respectively; M^{+} refers to a generic monovalent interlayer cation (equivalent numbers of cations of different valence may be indicated by $M^{n+}_{x+y/n}$).

Montmorillonite, beidellite and nontronite are di-octahedral smectites whereas saponite and hectorite are tri-octahedral smectites. In general, smectites may be differentiated according to a)

the di- or tri-octahedral nature of the octahedral sheet, b) predominant octahedral cation; and c) the density and location of the layer charge.

When the tetrahedral and octahedral sheets are joined in a layer, the resulting structure can be either electrically neutral or negatively charged. Smectite clay minerals possess a negative permanent layer charge that arises from cation substitutions in the phyllosilicate sheets: (i) substitution of Al^{3+} for Si^{4+} in tetrahedral sites; (ii) substitution of Al^{3+} for Mg^{2+} or lower charge cations in octahedral sites, and (iii) the presence of vacancies.

These substitutions lead to a positive charge deficiency, compensated by the presence of hydrated exchangeable cations in the interlayer space (Ca^{2+}, Mg^{2+}, Na^{+}, K^{+}, etc.). The total layer charge (LC) of a clay is the sum of the tetrahedral (T) and octahedral (O) charge.

Smectites are characterized by low layer charge, which varies from 0.25*e* to 0.60*e* per $O_{10}(OH)_2$ half unit cell (where *e*, the electron charge, is $1.6 \cdot 10^{-19}$ C).

Layer charge significantly affects the properties of 2:1 phyllosilicates [24,25,26], especially cation and water retention. The low charge of smectites implies a quite large cation exchange capacity (CEC) for these clays, because the bonds between the clay surface and interlayer cations are relatively weak. Furthermore, this low layer charge favours that the polar neutral molecules (such as water) can enter the interlayer producing swelling. By contrast, in high charge clays (as mica or chlorite), interlayer cations are much more strongly linked to the layer surface, therefore not always exchangeable. This property helps to strongly bond the layers together and the collapse of the structure can occur, especially in the presence of interlayer ions as K^{+} (typical interlayer ion for a 2:1 clay illite), with a consequent loss of the expansion capacity by absorption of polar molecules.

Most of the smectite layer charge is due to the permanent charge but a small additional contribution (generally < 5%) comes from the amphoteric functional groups at the edges of the clay particles (variable charge), where Si–O–Si and Al–O–Al bonds are broken and may convert into Si–OH (silanol) and Al–OH (aluminol) groups (Figure 1) [27]. These surface groups, generally named S-OH, are positively charged at acid pH ($S\text{-}OH_2^{+}$) and negatively charged at basic pH ($S\text{-}O^{-}$) and contribute to different arrangements of clays by the formation of edge-edge (EE) or edge-face (EF) aggregates, which are relevant in relation to other clay properties which may depend on pH and also in the stability of clay colloids.

The surface potential at these edges is related to the pH of the ambient solution, and the proton concentration at the point of zero charge (PZC) of the edge surface [28, 29].

The theoretical charge density (σ_0, in $C \cdot m^{-2}$) of the clay can be calculated from the interlayer charge and the unit cell parameters along the *x* and *y* axis (*a* and *b*), according to the formula of equation (3):

$$\sigma_o = \frac{e \times \text{interlayer charge}}{2(a \times b)} \qquad (3)$$

where, *e* is the electron charge ($1.6 \cdot 10^{-19}$ C) and *a* and *b* the unit cell parameters along the xy plane.

For instance, the charge density for phyllosilicates with tetrahedral charge usually varies between families, being 0.15 $C \cdot m^{-2}$ for beidellite, 0.34 $C \cdot m^{-2}$ for muscovite and to 0.7 $C \cdot m^{-2}$ for margarite (a brittle mica) [2]. In the case of smectites the charge density varies approximately between 0.15 to 0.7 $C \cdot m^{-2}$ (-0.07 to -0.21).

Apart from the degree of substitution, which give rise to different values of the total layer charge and charge density, the position of the substitutions (in O or T layer) may play a significant role on the overall behaviour of the clays [30,31,32].

With tetrahedral substitution, the negative charge resides on the three basal oxygens of the aluminate tetrahedral whereas if octahedral substitution is present, the negative charge resides on ten basal oxygens, five on either side of the layer [33]. Therefore, tetrahedral charge is much more localized than octahedral charge. This means that exchangeable cations are expected to be more tightly held to the surface if the permanent charge is predominantly located in the tetrahedral layer [34]. The localisation of the permanent charge can also affect particle-particle interactions. It has been reported, for example, that EF attraction is enhanced by tetrahedral charge [28].

In smectites, the negative layer charge (LC) ranges from 0.2 to 0.6 $mol_c \cdot mol^{-1}$, calculated based on their structural formulae (i.e., $O_{10}(OH)_2$ per half unit-cell content, *p.h.u.c*). In vermiculites (commonly tri-octahedral) the LC ranges between 0.6 and 0.85 $mol_c \cdot mol^{-1}$ and in micas between 0.6 and 1.0 $mol_c \cdot mol^{-1}$ (brittle micas up to 2.0). Layer charge significantly affects the properties of 2:1 phyllosilicate [35,36,37], especially cation and water retention. Smectites with a low charge of 0.2-0.6 $mol_c \cdot mol^{-1}$ have a quite large cation exchange capacity (CEC) because the bonds between the clay surface and interlayer cations are relatively weak, and favours that the polar neutral molecules (such as water) can enter the interlayer producing swelling. Vermiculites have a higher layer charge and, consequently, a higher cation exchange capacity than smectites. However, vermiculites do not swell in water as extensively as smectites, because most of the layer charge of vermiculite is located in the tetrahedral sheet. This fact promotes the exchangeable cations to electrostatically pull the layers together, increasing energy, diminishing layer separation (up to only two molecular sheets of water between the layers, producing a characteristic c-axis spacing of 14 Å, being lower than 17 Å of smectites).

Therefore, in high layer charge clays (as micas: 0.6-1 $mol_c \cdot mol^{-1}$ or vermiculites: 0.6-0.85 $mol_c \cdot mol^{-1}$) interlayer cations are linked strongly to the layer surface and therefore not always exchangeable, making stronger the layers bond. This effect may favour the collapse of the structure, especially in the presence of interlayer ions as K^+ (the case of illite), with a consequent loss of expansion capacity due to absorption of polar molecules. The selectivity of the clay minerals for K acts in the order: illite > vermiculite > smectites.

Depending on permanent charge location, smectites can be classified in different groups:

- Montmorillonites, in which the layer charge is provided by the octahedral sheet. They are classified as di-octahedral smectites with layer charge (LC) ranging from low to high. Low charge montmorillonites have a LC between 0.20-0.33 and high charge montmorillonites between 0.33-0.60.

- Beidellites, in which the layer charge is provided by the tetrahedral sheet. They are classified as di-octahedral smectites with LC from 0.20-0.33 for low charge beidellites and 0.33-0.60 for high charge beidellites.

- Nontronites, Fe-rich di-octahedral smectites with substitutions mainly in the tetrahedral layer.

- Saponites, in which the layer charge is provided by the tetrahedral sheet, are classified as tri-octahedral smectites with different LC.

- Hectorites and stevensites, in which the layer charge is provided by the octahedral sheet They are classified as tri-octahedral smectites where Li+ ions or vacancies replace Mg^{2+} divalent cations at octahedral sites, respectively.

Another important property of smectite is the type of interlayer cation being especially important their size and their hydration energy. Interlayer cations are reported to influence several physical properties of the clay minerals [38] including hydration and swelling [39].

Indeed, the distance between TOT layers in a clay mineral depends on the interlayer cation, changing the d(001) basal spacing: 9.6 Å for K-smectites; 12.5 Å for Na-smectites and 15.5 Å for Ca-Mg-smectites at low relative humidity or water activity. At high water activities the maximum hydration state of di- and tri-octahedral smectites becomes infinite for Na^+ and Li^+, 3-water layers for divalent cations and 2-water layers (octahedral charge) or 1-water layers (tetrahedral charge) for potassium.

The "double layer" generated by different cations around the clay particles is also different. Na^+ is preferentially distributed over the particle surface whereas Ca^{2+} ions are preferentially located in the interlayer , a process known as *demixing* [40].

Finally, it is well-known that the Na content in the exchange complex affects clays dispersion. The presence of Na in the interlayer (approximately above 20%), causes disaggregation of clay platelets and the formation of smaller tactoids [41,42,43]. Kaufhold and Dohrmann [44] analysed the capacity of different bentonites to release particles in diluted systems and concluded that Na-rich bentonites released far more colloidal particles than Ca/Mg-rich bentonites. Additionally, they found a relation between the Na^+ content and pH, which is also another relevant parameter in relation to colloidal properties.

1.3 COLLOIDS

Particles dispersed in a fluid with a size smaller than 1 µm are defined as "colloids". Smectite particles are colloidal under many chemical conditions. The main important property of colloids is their extremely small size, which confers them a large surface per unit mass, then high surface area (SA) and reactivity. In the case of smectite, in addition to the external surface of the particle, (large) internal surface between plates exist. This surface is not accessible to N_2 and can be measured only with polar gases (water vapour). For montmorillonite, a theoretical value of the total surface area of approximately 700-750 $m^2 \cdot g^{-1}$ is predicted from dimensions of the lattice structure [2].

Another important colloidal property is the surface charge, which governs many phenomena related to colloids. The colloid charge mainly depends on the pH and ionic strength of the fluid; it generates an electrical potential at the particle/water interface, which is generally repulsive when two particles have charges of the same sign. If colloids repel each other the suspension remains stable. If the magnitude of the charge and consequently the repulsive potential decreases (for changes in water chemistry, adsorption processes, etc.) colloids coalesce and form aggregates. The reverse process of the breaking up of aggregates into smaller or individual particles is known as *de-flocculation* or *dispersion*.

Stability studies analyse whether aggregation occurs depending on several chemical and physical parameters, such as pH, ionic strength, presence of different multivalent ions, organic ligands or temperature, amongst other factors. Less attention was paid so far to the effects of the intrinsic physicochemical properties of the clays on their stability.

In a HLWR repository the hydration of the clay surface promotes the release of bentonite colloids [12, 22, 45].

To be relevant in RN transport, colloids must exist in a non-negligible concentration, be stable and mobile and be able to adsorb RN irreversibly [46]. In particular, the presence of mobile colloids may favour the migration of radionuclides that present low solubility and are fairly immobile.

The analysis of the role of colloids in radionuclide transport is still an issue for the performance assessment (PA) of a DGR.

The contribution of bentonite colloids to RN migration is being studied in depth, because of their possible relevance on the RN-facilitated transport in crystalline fractured rock [47, 48, 49].

The main objective of this study is to compare the main colloidal properties of different smectites: to understand them in-depth and to determine the possible implications on erosion processes of the engineered barriers in radioactive waste repositories.

2 MATERIALS AND METHODS

2.1 CLAY MINERALS

Different clays were selected for this study. Most of them are bentonites, which have been largely studied in the frame of international projects related to HLRW. Three commercial di-octahedral smectites were obtained from the Clay Minerals Society Source Clays Repository (SBId-1, NAu1, SAz-2) another one was supplied by NANOCOR® (China). Additionally, two different saponites (B64, MCA-C) were also included in the study.

Other clayey materials were also investigated, even if with less detail so far. Furthermore, some experiments described in this work were also carried out with the clays exchanged with Na or Ca.

The selected bentonites are the following:

- **FEBEX** bentonite mined in the Cortijo de Archidona, Almería, Spain [50,51,52].
- Bentonite from **Milos** Island in Greece [53]. The Milos bentonite is mined by Silver & Baryte Mining Company S.A. Its commercial name is IBECO (the sample under study is IBECO RWC 16).
- Wyoming **MX-80** bentonite from USA produced by Am. Coll. Co [54].The Wyoming type of bentonite occurs as layers in marine shales, and is widespread and extensively mined, not only in Wyoming but also in parts of Montana and South Dakota.
- Three Czech bentonites extracted from the Rokle deposit, in the Kadan basin, c. 100 km WNW of Prague. The bentonite from this deposit is highly variable in colour, ranging from olive-gray to yellow/red due to the admixture of secondary iron and manganese oxides.The clay referred as to **Rokle-S65** (Sabenil) is a fully Na-activated commercial clay [55]; the **Rokle-B75** is a partially Na activated clay and the **Rokle-F0** is untreated.
- Russian bentonite from the Khakassia deposit [56]. This clay is named **MSU** (the name given by the acronym of the Moscow State University).

The selected commercial di-octahedral smectites are:

- **NANOCOR®** (China), that is a Na-exchanged and purified *montmorillonite*.
- **SBId-1** (Clay Mineral Society): it is a *beidellite from* Idaho (USA) [57].
- **NAu-1** (Clay Mineral Society): it is a *nontronite* i.e a ferruginous (4.50 mmol Fe g^{-1}) smectite coming from from the Uley Graphite Mine in South Australia [58].
- **SAz-2** (Clay Mineral Society): also known as “Cheto” clay [59], it is mined in the state of Arizona (USA)

Finally, the two tri-octahedral smectites (saponites) are:

- **Saponite B64:** a Mg-Fe smectite from the Ventzia continental basin at east of Grevena in Macedonia, Greece [60, 61].

- **Saponite MCA-C:** a Mg-smectite from Cerro del Aguila-Cerro del Monte from the Cuenca de Madrid Basin, Spain [62].

Some tests reported here were made with Ypresian clays material [63-64]. Ypresian Clays is a relatively thick sequence of dominantly fine-grained sediments deposited early in the Eocene (about 54 to 51 million years ago). The bulk mineralogy of the Ypresian clays is composed of 25%-65% of clay minerals and 35%-75% of non-clay minerals (mainly smectite and illite and in lesser extent chlorite and kaolinite).

The two Ypresian clays analysed were:

- **DOEL-40**: This core sample (378.78-379.58 m depth) from the Roubaix-Moen Member belongs ON-Doel borehole drilled in 1998 in the Doel nuclear zone, (Antwerpen, Belgium).

- **KALLO-38**: This core sample (324.89-325.84 m depth) from the Roubaix/Moen member belongs to ON-Kallo borehole drilled in 2009 in the Kallo town (Beveren, Belgium).

High-quality commercial bentonites normally contain over 80% of montmorillonite, which is expected to give various bentonite products similar sealing properties. However, other minerals in raw bentonite may vary, also in different batches. Typical accessory minerals are feldspars, quartz, cristobalite, gypsum, calcite and pyrite. The accessory minerals, other phyllosilicates and other substances such as organic matter may affect the overall properties of the material.

The samples were used “as received” and some of them were also exchanged with Na or Ca. In order to homoionise the clays, they were washed three times with the respective Na / Ca electrolyte (1 M $NaClO_4$ or $Ca(ClO_4)_2$) and then washed with deionized water (DW) and finally with DW/ethanol until the electrical conductivity of the suspension was lower than 50 $\mu S \cdot cm^{-1}$. Afterwards, the homoionic clays were dried in the oven and powdered in an agate mortar.

2.2 CLAY CHARACTERIZATION

A complete geochemical and mineralogical characterization was carried out by different techniques (XRD, FRX, FTIR, TG-DSC, etc.,) to evaluate major and minor minerals, clays content, cation exchange capacity, major cations, water content, pore water chemistry, BET and total surface area, layer charge distribution and unit cell formula. All the details of this work can be found elsewhere [51]. Here, we will give only a summary of the methodologies used.

To identify the main minerals, present in the clay rock samples, XRD analyses were carried out, and complemented with TEM-EDS, TG-DSG, and FT-IR analyses. The chemical composition of the samples was determined by X-ray fluorescence. The total CEC was measured with 0.01 M copper

tri-ethylenetetramine (Cu-Trien) method; the determination of the main exchangeable cations was carried out using Cs or Co as index cations [65]. The external BET surface area was determined by using classical nitrogen adsorption/desorption isotherms, whereas the total surface area was determined by water vapour adsorption measurements by storing the samples at a constant 75% relative humidity atmosphere in a desiccator over-saturated in NaCl solution for 1 month.

Karland and Birgesson [66] pointed out some problems regarding the determination of structural parameters for raw clays (charge distribution, for example), especially related to the presence of oxides (i.e., titanium oxide). In fact, the identification of such minerals by XRD is not possible if their grain size is too small. Titanium could occupy sites both in the octahedral (preferably) and in the tetrahedral layers, thus whether Ti is included in the structure or not may affect charge distribution calculation. The same authors reported that in the Rokle clay, with a very high Ti content, the charge changed from 85% in tetrahedral position to 32% by including or not titanium.

2.3 WATER CHEMICAL ANALYSES

Water samples in contact with the clays were filtered through 0.2 μm filters. Measurements of pH (± 0.10) were made using a Mettler Toledo (S220) pH-meter with a solid polymeric electrode (Xerolyt) or a Crison pH-ion meter (GLP225) with a combined glass pH electrode (Metrohm). Electrodes calibration was made with buffer solutions at pH 2.00, 4.00, 7.00, and 10.00. Conductivity measurements were carried out with a Crison EC Meter Basic 30^{+}.

Major and trace cations were analysed by inductively coupled plasma atomic emission spectrometer (Varian 735ES, AA240 FS). Sodium and potassium were determined by flame atomic emission spectrometry (Perkin Elmer 2280). Anions were analysed by ion chromatography (DIONEX ICS-2000). Carbonates were determined by titrations (METRHOM MOD796).

2.4 CLAY COLLOIDS

2.4.1 PREPARATION OF COLLOID SUSPENSIONS

Colloids were extracted from the different as received or exchanged clays by dispersing them (1 g/L) in deionized water (DW) and collecting the supernatant upon centrifuging at approximately 700·g during 10 min. This centrifugation procedure aimed to eliminate particles with size larger than 1 μm. The quantity of colloids dispersed from the bulk clay in each case was measured by gravimetric measurements, after drying the suspension (50 mL, per triplicate) at 90 °C in an oven. DW was used to maximize clay colloid dispersion, under the given centrifugation conditions. The *"(maximum) mass of dispersed particles"* can be considered the first clay intrinsic property to be considered.

The initial conductivity and pH of colloid suspensions were measured. A relatively low solid to liquid ratio was used to minimize the possible effects of soluble salts present in the clay on the solution chemistry. However, under these experimental conditions, some clay dissolution may occur. The water in equilibrium with the colloidal phase after filtering (by 0.2 μm) was analysed to determine the presence of different types of ions leached from the clays.

2.4.2 COLLOID SIZE

The size of colloids was measured by dynamic light scattering with a Malvern NanoS apparatus with He-Ne laser and at a measurement angle of 173°.

The size of clay colloids in the initial suspension, upon having centrifuged 1 $g \cdot L^{-1}$ of clay at 700·g, 10 min was measured first. As, under the selected conditions, the effect of water chemistry is minimized, the "*initial colloid size*" can be considered as an intrinsic colloidal property of the clay. This parameter will be related afterward to other physicochemical characteristics.

In a second step, the stability of extracted colloids was examined observing the particles aggregation upon progressive additions of Na^+ or Ca^{2+}. The concentration of monovalent or divalent cation needed to start coagulation process (critical coagulation concentration, CCC) was thus determined for each clay, at the initial pH of the suspension.

The onset of coagulation was assumed when the mean size of the particle was incremented of approximately a 20% in respect to the initial size. The concentration of ions (Na or Ca) needed to bring the particles out from the colloidal range (1 μm) was also determined.

2.4.3 COLLOID SURFACE CHARGE

In parallel to colloid size measurements, colloid surface charge was analysed through measurements of the particle mobility and calculation of ζ-potential (zetapotential).

According to the Gouy-Chapman theory of the electrical double layer, the relationship between the surface charge density (σ) and the surface potential (ψ) is given (for a symmetric electrolyte) by:

$$\sigma = \sqrt{8n\varepsilon kT}\sinh\left(\frac{ze\psi}{2kT}\right) \qquad (4)$$

where n is the bulk concentration of ions of valence z, ε the permittivity, k the Boltzmann constant, T the temperature and *e* the electron charge.

The zetapotential represents the potential produced by the double layer near the electrolyte/particle interface at the location of the "slipping plane", which limits the layer of fluid adhered to the particle moving with it. Thus, the zetapotential is not exactly equal to the surface potential generated by the surface charge of the particles but it is often the only possible mean to characterize surface charge at least in terms of sign and magnitude [67]. The zetapotential can be estimated by electrophoresis techniques, measuring the velocity and direction of charged particles under a given electric field. *i.e.* evaluating their electrophoretic mobility, U_E. The electrophoretic mobility is the velocity of the particles ($m^2 \cdot s^{-1}$) divided by the magnitude of the electric field (in V).

The mobility is converted to the zetapotential considering the properties of the fluid (dielectric constant ,ε, and viscosity,η) and different theoretical approximations [67]. The Henry expression relates the electrophoretic mobility to the zetapotential according to the following expression:

$$U_E = \frac{2\varepsilon\zeta f(\kappa a)}{3\eta} \quad (5)$$

In equation (5), f(κa) is the Henry function, which varies from 1 to 1.5.

The most known theory to calculate zetapotential from mobility data is the Smoluchowski approximation. In that case, f(κa)=1.5 and Equation (1) is equivalent to the Helmoltz-Smoluchowski equation [67]. The Smoluchowski approximation is valid only when the Debye length (1/κ) is much smaller than the particle radius (a), therefore it is adequate for particles larger than about 0.2 μm and dispersed in electrolytes containing more than 10^{-3} molar salt.

This condition can be expressed as: κ·a >> 1 where

$$\kappa = \sqrt{\frac{\sum_i e^2 z_i^2 n_i}{\varepsilon k T}} \quad (6)$$

In equation (6), *e* is the charge of the electron z_i is the valence of the ion *i* present in the electrolyte, k is the Boltzmann constant, T the absolute temperature, n_i the number concentration of the ion I and ε ($\varepsilon_r \cdot \varepsilon_0$) the absolute permittivity.

In the other cases, when κ·a is not >> 1, this approximation is not valid and other theories must be considered.

As the initial salinity of the colloid suspensions water was very low (clay colloids were dispersed in DW), the Smoluchowski approximation could not be always used. Thus, a reference ζ-potential value will be given, corresponding to the measurement obtained after adding to the initial colloid suspension 1 mM of Na. At this Na concentration, κ·a values are approximately 20 and the Smoluchowski approximation can be applied.

Particle mobility was measured by Laser Doppler Electrophoresis with a Zetamaster Malvern system equipped with a 2 mW He-Ne laser (λ = 633 nm). The mobility of clay colloids was also measured upon progressive additions of Na^+ or Ca^{2+} to determine their stability as a function of the ionic strength.

2.4.4 COLLOIDS MICROSTRUCTURE

After having prepared the colloidal suspensions, they were filtered by 0.2 μm, in order to collect the water for chemical analyses. The material collected in the filters was observed by Atomic Force Microscopy in tapping mode, with a Nanoscope IIIa apparatus (Digital Instruments). AFM image analysis was carried out with the WSXM 4.0 software [68].

3 RESULTS AND DISCUSSION

3.1 CLAY CHARACTERISATION

Table 1 shows a summary of the main characteristics of the clays studied in this work. In particular, the following parameters are evidenced: the content of smectite; the content of Na and main divalent ions (Ca + Mg) in the exchange complex, the total layer charge and its distribution between the octahedral and tetrahedral layer, the charge density, the surface area (BET and total) and the total CEC.

The clay with the lowest total layer charge is the MX-80, which presents only octahedral substitutions, like the commercial NANOCOR®. These two clays are basically Na-type clays. In contrast, the smectite with the highest total layer charge is the Cheto clay, which also presents predominantly octahedral substitutions but is a Ca-type smectite.

Beidellite and nontronite (SBId-1 and NAu-1) have relatively high layer charge and substitutions mainly in the tetrahedral layer; both are Ca-type clays.

The two selected tri-octahedral smectites (Saponite B64 and MCA-C) are Mg-type clays having a similar total layer charge. However, the charge distribution is predominantly tetrahedral in MCA-C, as in a perfect saponite, and predominantly octahedral in B64.

KALLO and DOEL clay rocks have only a small amount of smectite (< 50%), therefore they will not be studied in detail; they will be basically used to understand the role of smectite mineral in clay rocks on colloid generation. Other two clays, the Czech Rokle-F0 and the saponite B64 have relatively low smectite content (≤70%), are also less relevant for this study.

Another important point that may affect the stability of colloids is the quantity of soluble salts naturally present in the clay, especially at high solid to liquid ratio, which may increase the salinity of the groundwater near the bentonite. In the present experiments, the effect of water chemistry and clay/water interactions is somewhat lessened on purpose to maximise generation and to minimise coagulation, but in previous erosion studies performed under the frame of the European BELBAR project, it was found that salinity higher than 10-20 mM (Na) may completely inhibit the erosion process [69,70].

Thus, this is a point to account for in the overall discussion of the properties affecting bentonite erosion under repository conditions.

A higher amount of soluble salts (either naturally or due to other treatments) will especially affect the chemical characteristics of the water in contact, when present at high solid to liquid ratio. The anion inventory (Cl- and SO42-) was determined by aqueous leaching at 1:8 solid to liquid ratio in the studied clays and the results are summarized in Table 2.

Clay	Sm	Na Exch (%)	Ca + Mg Exch (%)	Tet. Charge	Oct. Charge	Total Layer charge	Charge Density	BET ($m^2 \cdot g^{-1}$)	SA ($m^2 \cdot g^{-1}$)	CEC (Cu-Tri)
FEBEX	94	28.0	66.4	-0.07	-0.41	-0.48	0.16	59.2	628	98.1
IBECO	88	26.3	69.0	-0.04	-0.29	-0.33	0.11	70.8	611	90.2
MX-80	89	68.3	26.3	-0.08	-0.2	-0.28	0.1	39.6	481	83.6
Rokle-F02	70	0.8	92.8	-0.21	-0.09	-0.30	nd	82.8	573	73.8
Rokle-B75 (part. act.)	78	55.7	34.6	-0.29	-0.11	-0.40	0.14	77.2	396	60
Rokle-S65 (fully act.)	78	76.9	16.7	-0.26	-0.11	-0.37	0.13	109.7	526	72.9
MSU	79	90.2	4.5	-0.14	-0.21	-0.35	0.12	22.3	442	68.2
NANOCOR®	98	89.2	7.5	-0.04	-0.34	-0.38	0.13	23	575	86.9
SBId-1 (Beidellite)	78	0.7	92.0	-0.26	-0.06	-0.32	0.11	33.7	337	52.8
Nau-1 (Nontronite)	90	3.8	91.3	-0.32	-0.05	-0.37	0.12	57.8	622	85.8
SAz-2 – Cheto	98	0.4	92.3	0.00	-0.5	-0.50	0.17	93.5	790	107
MCA-C (Saponite)	78	4.2	87.9	-0.25	-0.15	-0.40	0.13	136	558	59.7
B64 (Saponite)	65	0.3	92.3	-0.13	-0.38	-0.51	0.17	141.4	596	58.6
DOEL-40	26	47.6	34.1	-0.14	-0.24	-0.38	0.13	52.2	187	31.1
KALLO-38	30	56.9	30.5	-0.14	-0.26	-0.40	0.14	57.9	160	33.3

Table 1. Main physico-chemical characteristics of the raw clays used in this study

Sample	Cl^- mmol/100g	SO_4^{2-} mmol/100g
FEBEX	3.01	0.78
IBECO	1.82	1.35
MX-80	1.36	3.26
Rokle-F02	1.26	0.09
Rokle-B75 (part. act.)	1.21	0.11
Rokle-S65 (fully act.)	1.27	0.07
MSU	2.06	1.82
NANOCOR®	4.4	10.68
SBId-1 (Beidellite)	1.29	0.15
Nau-1 (Nontronite)	2.87	0.08
SAz-2 - Cheto	1.32	0
B64 (Saponite)	1.5	0
MCA-C (Saponite)	1.56	0.09
DOEL-40	5.05	0.66
KALLO-38	1.62	1.31

Table 2. Anion inventory of the raw clays.

The NANOCOR® clay, for example, has especially high Cl^- and SO_4^{2-} content compared to the other analysed clays, probably due to the treatment performed for purifying/exchanging it. Relatively high sulphate content is also present in the MX-80 and MSU. DOEL-40, NAu-1 and FEBEX show a chloride content slightly higher than the other clays.

3.2 INITIAL PROPERTIES OF CLAY COLLOID SUSPENSIONS

3.2.1 CONTACT WATER CHEMISTRY

The characteristics of supernatant of the different colloid suspension (upon filtering by 0.2 µm) are summarized in Table 3 and Table 4, respectively. The first measurement consisted of the determination of pH and conductivity of the suspensions. pH values range from 7 to 9.5 and the electrical conductivity from 10 to 90 $\mu S \cdot cm^{-1}$ approximately.

This is a first indication that a different quantity of ion leached from the clays is present. The analysis of the main anions and cations present in the initial suspension is also indicated in the tables.

Significantly higher values of Na are observed for MCA-C, and NANOCOR® followed by Rokle-F0 and MSU. NANOCOR® and MX-80 also show the highest concentration of Al, which could be symptom of some clay dissolution as hydrolysis of clay in contact with deionized water cannot be ruled out.

The initial calculated ionic strength indicated very low salinity in all the initial suspensions, with a maximum for NANOCOR® and MCA-C (around $1 \cdot 10^{-3}$ M) and minimum for the beidellite ($9 \cdot 10^{-5}$ M). Thus aggregation effects for ionic strength in the initial sample would be limited.

Sample	pH	Cond	Al $mg \cdot L^{-1}$	Ca $mg \cdot L^{-1}$	Cl $mg \cdot L^{-1}$	Fe $mg \cdot L^{-1}$	K $mg \cdot L^{-1}$	Mg $mg \cdot L^{-1}$	Na $mg \cdot L^{-1}$	SO_4^{2-} $mg \cdot L^{-1}$	Ti $mg \cdot L^{-1}$	I (M) $*10^{-4}$
FEBEX	8.8	25.2	0.04	0.00	1.10	<0.03	0.0	<0.03	5.8	1.6	<0.03	3
MILOS	8.9	44.8	0.07	0.00	0.85	0.11	1.0	0.06	4.3	2.8	<0.03	3
MX-80	9.4	56.8	<0.03	2.00	0.76	<0.03	1.0	0.69	5.5	2.1	<0.03	5
Rokle-F02	8.1	51.2	<0.03	3.00	<0.1	<0.03	1.0	1.00	7.5	0.1	<0.03	6
Rokle-B75 (par. Act.)	7.2	21.3	0.06	1.00	0.15	0.09	1.0	0.32	0.5	0.1	<0.03	2
Rokle-S65 (fully act.)	9.1	10.9	<0.03	2.00	<0.1	<0.03	1.0	0.71	1.4	<0.1	<0.03	3
MSU	8.7	28.5	6.10	0.00	0.35	1.60	0.0	0.96	6.1	4.7	0.04	5
NANOCOR®	7.8	40.9	17.00	0.00	1.30	4.60	0.0	2.40	11.0	12.0	0.11	11
SBId-1 (Beidellite)	8.4	14.1	<0.03	0.00	0.10	<0.03	<0.1	<0.03	0.2	<0.1	<0.03	1
NAu-1 (Nontronite)	7.6	29.7	<0.03	<0.03	0.45	<0.03	0.0	<0.03	1.0	<0.1	<0.03	1
SAz-2 – Cheto	8.5	14.0	<	0.00	0.21	<	0.0	0.07	0.7	<	<	1
B64 (Saponite)	6.8	81.6	<0.03	1.00	0.21	0.04	0.0	1.50	0.2	<0.1	<0.03	3
MCA-C (Saponite)	9.6	73.3	0.18	1.00	0.75	0.07	1.0	0.34	22.0	1.7	<0.03	11
DOEL-40	9.0	42.7	<0.03	5.00	1.70	<0.03	1.0	0.25	4.9	0.9	<0.03	nd
KALLO-38	7.3	7.1	nd	nd	nd	nd	nd	nd	nd	nd	nd	nd

Table 3. Chemistry of the supernatant of the colloidal suspensions from as-received clays, filtered by 0.2 µm.

Sample	pH	Cond	Al $mg \cdot L^{-1}$	Ca $mg \cdot L^{-1}$	Cl $mg \cdot L^{-1}$	Fe $mg \cdot L^{-1}$	K $mg \cdot L^{-1}$	Mg $mg \cdot L^{-1}$	Na $mg \cdot L^{-1}$	SO_4^{2-} $mg \cdot L^{-1}$	Ti $mg \cdot L^{-1}$	I (M) $*10^{-4}$
FEBEX-Ca	6.8	14.2	<0.03	2.40	0.10	<0.03	0.3	0.06	0.3	<0.1	<0.03	2.25
FEBEX-Na	7.0	11.6	0.04	0.88	0.25	<0.03	<0.1	0.06	2.5	0.3	<0.03	2.13
MCAC-Na	9.5	16.9	0.08	0.15	0.30	<0.03	0.1	0.43	5.9	<0.10	<0.3	-
MILOS-Ca	7.6	32.1	<0.03	5.50	0.20	<0.03	0.2	0.17	<0.1	0.2	<0.03	4.14
MILOS-Na	9.2	89.1	<0.03	16.00	0.32	<0.03	0.3	1.30	12.0	1.8	<0.03	8.4
MX-80-Ca	9.2	14.2	<0.03	2.00	0.31	<0.03	<0.1	0.06	0.3	0.5	<0.03	1.82
MX-80-Na (*)	8.8	12.2	70.00	1.70	0.44	18.00	0.7	10.00	13.0	0.9	0.52	-
Rocke-S65-Na (*)	8.2	67.1	5.30	18.00	0.26	4.70	0.6	4.60	12.0	0.2	1.20	-
Rokle-B75-Ca	8.2	34.4	<0.03	5.50	0.12	<0.03	0.3	0.27	0.1	<0.10	<0.03	-
Rokle-B75-Na	7.9	32.0	<0.03	3.40	0.20	<0.03	0.5	0.65	1.3	<0.1	<0.03	-
SBId-1-Na	8.4	14.1	<0.03	0.31	0.26	<0.03	0.2	<0.03	0.7	<0.10	<0.03	1.65

Table 4. Chemistry of the supernatant of the colloidal suspensions from exchanged clays, filtered by 0.2 µm (not filtered).*

The highest concentration of sulphates is also observed in NANOCOR® and MX-80 suspensions, according to the anion inventory of these clays. Other large differences on chemistry cannot be detected in the initial suspensions.

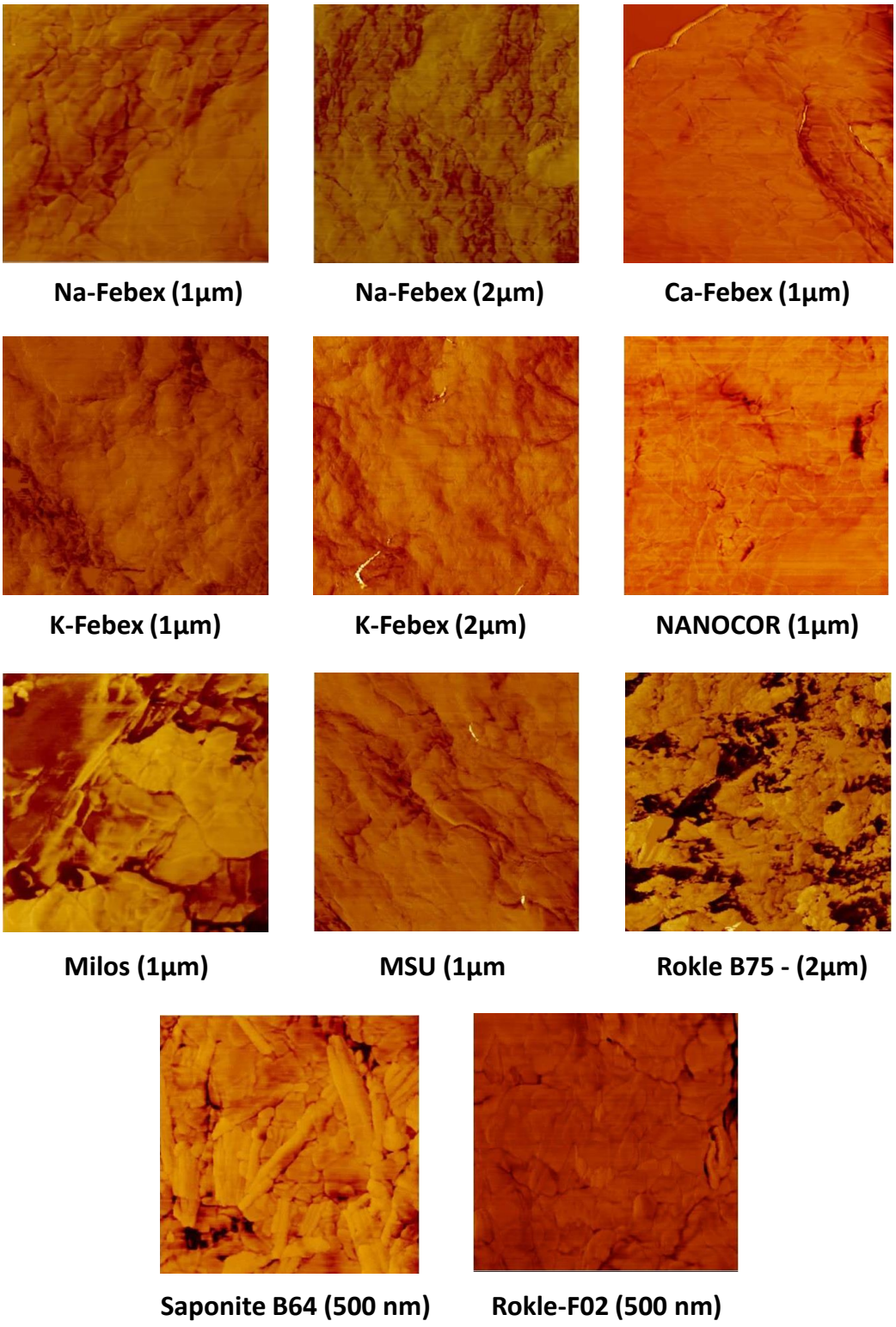

Figure 2. AFM Images of some of the analysed clay. Below the image, the name of the sample and the dimensions of the image (square size).

3.2.1 ANALYSIS OF COLLOID MICROSTRUCTURE BY AFM

Figure 2 shows a selection of the AFM images taken on some of the clays under study. Under the picture, the name of the sample and the size of the analysed image are given. In general, tri-octahedral smectites look like compacted flakes, with similar morphology. The raw clays show aggregates rougher than the homoionised ones, especially than Na-clays Saponite (B64) flakes are

more similar to sticks. The Rokle-F02 sample presents small particles than can correspond to minerals others than clay, especially oxides, which can make more difficult the analyses of the colloidal properties of the clay.

3.2.2 SUMMARY OF DATA

Table 5 shows the summary of the main characteristics of the colloids extracted from the different as-received clays. Table 6 shows the same parameters determined for the exchanged clays. These parameters will be discussed: (a) the concentration of colloid dispersed from the clay, presented in *parts per million* (ppm) either normalized or not to the smectite content of the clay); (b) the initial particle size; (c) the initial mobility and d) the particle zetapotential measured after the addition of 1 mM Na to the initial suspension (reference zetapotential).

CLAY	ppm	ppm/Sm	Size (nm)	MOBILITY (µm·s-1)/(V·cm-1)	ZetaPotential (mV) At 1 mM Na	ZetaPotential (mV) At 10 mM Na
FEBEX	166±15	176.60	349±1	-2.18±0.07	-33.4±1.6	-33.8±1.2
IBECO	157±11	178.41	367±5	-1.80±0.05	-26.2±0.9	-33.7±1.1
MX-80	178±12	200.00	336±2	-2.57±0.08	-35.1±1.1	-45.3±1.1
Rokle-F02	115±33	164.29	288±4	-1.43±0.04	-27.2±0.7	-33.6±0.8
Rokle-B75 (Par. Act)	124±6	158.97	378±9	-1.50±0.04	-24.5±1.8	-35.0±0.5
Rokle-S65 (Fully Act)	153±19	196.15	415±5	-2.00±0.06	-28.2±1.0	-31.7±0.7
MSU	263±7	332.91	304±8	-2.37±0.07	-32.0±0.5	-37.5±0.6
NANOCOR®	720±43	734.69	250±10	-2.96±0.09	-37.7±1.1	-41.3±0.6
SBId-1 (Beidellite)	49±15	62.82	700±100	-2.60±0.15	-32.9±1.9	-44.4±1.3
NAu-1 (Nontonite)	39±4	43.33	783±62	-2.30±0.11	-32.2±1.5	-37.4±0.9
SAz-2 – Cheto	61±20	62.24	550±100	-1.47±0.09	-21.8±1.7	-29.5±0.8
B64 (Saponite)	65±28	100.00	553±52	-1.05±0.03	-22.5±0.4	-29.7±1.4
MCAC (Saponite)	80±12	102.56	624±108	-1.01±0.13	-25.0±1.4	-30.4±0.9
DOEL 40	52±6	200.00	531±26	-1.23±0.04	-23.4±0.7	--
KALLO 38	51±6	170.00	250±50	-2.60±0.08	-31.9±1.6	--

Table 5. Main characteristics of the colloids generated in DW from the different clays. As-received clays.

CLAY	ppm	ppm/Sm	Size (nm)	Mobility (µm·s-1)/(V·cm-1)	ZetaPotential (mV) At 1 mM Na	ZetaPotential (mV) At 10 mM Na
FEBEX-Ca	47±7	50.00	600±15	-1.3±0.04	-25.6±1.0	-30.2±0.8
FEBEX-Na	321±37	341.00	260±10	-2.50±0.04	-33.2±0.8	-37.1±1.0
MILOS-Ca	71±5	60.00	649±40	-0.75±0.02	nd	nd
MILOS-Na	353±5	401.00	284±3	-2.30±0.07	-32.6±0.8	-38.7±1.0
MX-80-Ca	53±7	59.00	523±25	-1.18±0.03	-25.0±1.0	-36.4±0.6
MX-80-Na	600±50	674.00	249±10	-2.70±0.08	-35.3±0.9	-41.5±1.0
Rokle-S65-Na	394±20	505.00	437±10	-1.85±0.06	-28.9±1.0	-33.0±0.3
Rokle-B75-Ca	53±5	68.00	527±81	-0.84±0.03	nd	nd
SBId-1-Na	412±32	528.00	539±9	-2.71±0.08	-40.2±1.1	-47.1±2.8

Table 6. Main characteristics of the colloids generated in DW from the different clays. Exchanged clays.

3.3 ANALYSIS OF PARAMETERS AFFECTING COLLOID DETACHMENT

The first important data to be analysed is the mass of colloids obtained upon centrifuging, which provides the first indication on the capability of the different clays to disperse colloidal particles under the most favourable chemical conditions given by deionised water (DW). In the case of as-received clays (Table 5), NANOCOR® clay generated the highest quantity of colloidal clay particles, followed by MSU. Both are Na-type clays. The minor quantity of particles is generated by KALLO-40 and DOEL-38 clayrocks, which have the smallest smectite content, and by the nontronite (NAu-1) and SAz-2, which are naturally Ca-clays.

In the case of exchanged clays (Table 6), the Na-exchanged materials generated significantly higher quantity of colloidal particles than the respective Ca-exchanged. Thus, as expected, the capability of the material of releasing colloids is related to the composition of the exchanging cations. As already mentioned in the Introduction, Na is known to favour the dispersion of clays.

Therefore, to simplify the comparison of all the data, the clays were first classified considering the composition of their interlayer cations. *Na-type clays* will be defined those with Na>80% and Ca+Mg<10% in the exchange complex (blue triangles in the graphs); *Ca-type* those with Na<10% Ca+Mg>70% (black squares in the graphs); (Na-Ca) *mixed-type clays* the others with intermediate Na/Ca values (red circles in the graphs).

When the clays were homoionised, for simplicity, 100% of the exchanging cation was considered, unless the value was experimentally verified.

3.3.1 SMECTITE AND NA CONTENT

Figure 3 shows the mass of colloids generated as a function of the smectite content for a) Na-Clays; b) Na-Ca mixed-clays and c) Ca-Clays. The quantity of colloids generated from Na-clays (250 to 750 ppm) is higher than in Na-Ca mixed-clays (50 to 200 ppm) or Ca-clays (from 40 to 120 ppm).

Most of Ca-clay generates around 50 ppm of colloid mass; only the Rokle-F02 generates more than 100 ppm value comparable to that seen by Na-Ca mixed clays. The presence of colloids coming from clay impurities (oxides for example) may contribute to the measurements. Relatively small quantity of particles is generated from KALLO and DOEL clays, which even having relatively large quantity of Na in the exchange complex (48-57%), have quite low smectite content.

The mass of generated colloids increases almost linearly as the smectite content in the clay increases in Na- and Na-Ca mixed-clays; instead no such dependence is clearly observed for Ca-clays. Alonso et al. [71] in erosion experiments with compacted and confined clays, also observed a certain dependence on the colloid release with the smectite content.

As the quantity of smectite might be relevant on mass loss, a normalization of the mass of colloid generated in respect to the smectite content will be done (colloid mass in ppm /% Sm) for generalizing data and referring them to the main mineral of interest.

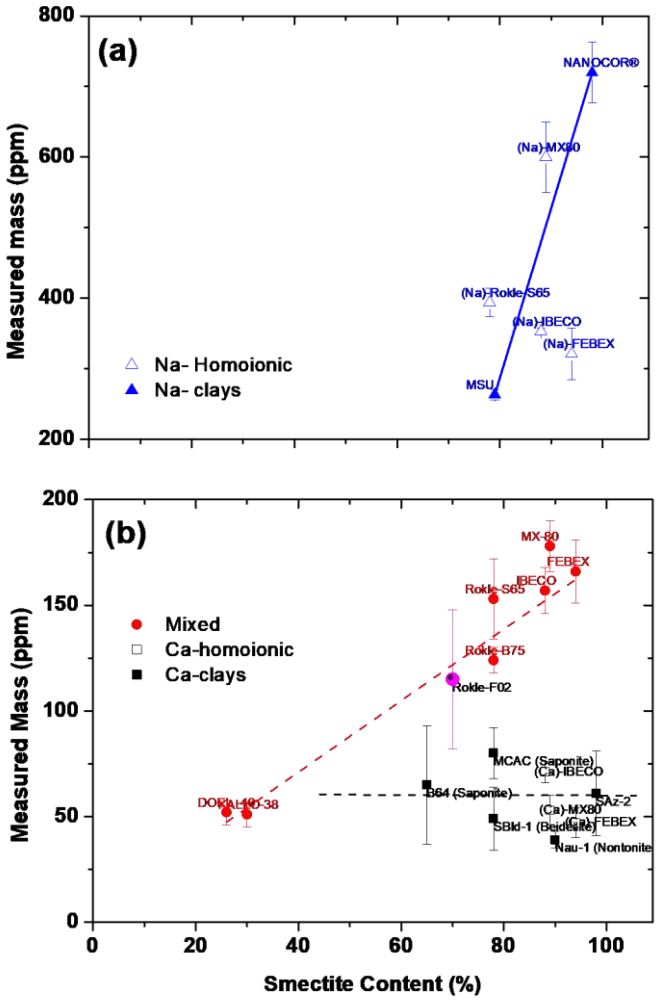

Figure 3. Mass of colloid generated as a function of the smectite content. (a) Na-Clays; (b) (Na, Ca)-mixed and Ca-clays. ◢ Na Clays; △ Homoionic Na-Clays; ● (Ca,Na)-mixed Clays; ■ Ca-Clays; □ Homoionic Ca-Clays.

Figure 4 shows the dependence of colloidal mass release (data normalized to the Sm content) on the quantity of Na (Figure 4a) or Ca+Mg (Figure 4b) in the exchange complex. Data are clearly distributed in three clearly defined zones: Na-clays released the highest colloidal mass (350-800 ppm); all the Na-Ca mixed- clays (with 20<Na<80) generated approximately the same quantity of colloids (150-250 ppm). The colloidal mass generated by Ca-clays (between 30-150 nm) is always lower than that of mixed clays. However, colloid mass generated in Na-clays is highly spread (from 350 to almost 800 ppm) and a certain spread is observed (from 40 to 120 ppm) also in Ca-clays. Therefore, apart from the Na/Ca content in the exchange complex, other factors must affect the higher/lower presence of colloids released in solution.

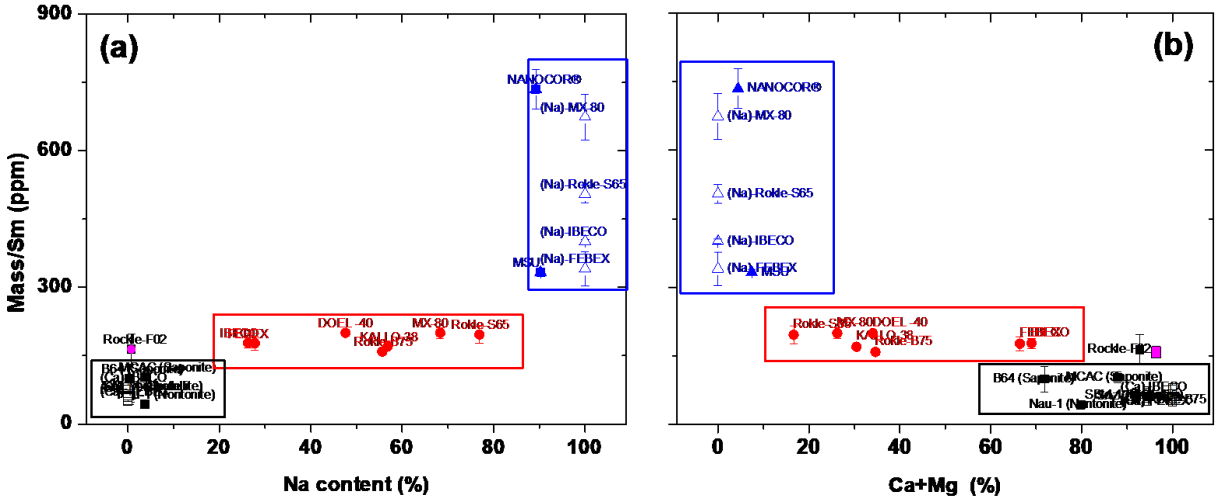

Figure 4. Mass of colloid generated normalized to the smectite (Sm) content as a function of (a) Na in the exchange complex; (b) Ca+Mg in the exchange complex. ◢ Na Clays; △ Homoionic Na-Clays; ● (Ca,Na)-mixed Clays; ■ Ca-Clays; □ Homoionic Ca-Clays.

3.3.2 LAYER CHARGE AND CHARGE DISTRIBUTION

The next parameter that will be investigated is the distribution of the permanent charge in the clays (tetrahedral, T *vs.* octahedral, O charge).

Figure 5 shows the generation data as a function of the percentage of tetrahedral charge of the different as received and homoionic clays. Figure 5a shows the mass generated normalised to the Sm content. In Ca- and mixed-clays a dependence on the distribution of the layer charge was not observed. Just as additional observation, the tri-octahedral saponites seem to generate a slightly higher quantity of colloids than other Ca-clays.

In Na-clays, the highest quantity of colloids is observed for NANOCOR® and Na-MX-80 which have a content of Na in the exchange complex higher than 95%, and high smectite content (>90%) and almost null tetrahedral charge. This means that, when the smectite interlayer cation is almost exclusively Na, a very low value of the tetrahedral charge will further favour the dispersion of smectite colloidal particles. (Almost) null tetrahedral charge and Na in the interlayer significantly decreases the interactions between the TOT units, this favouring colloid detachment. Sample MSU, should behave similarly to these two clays having null tetrahedral charge, but its lower smectite content (78%) is the factor that inhibits particle dispersion. Apart from the two abovementioned clays, the rest of Na-clays generates a mass of colloids perfectly ordered with the percentage of tetrahedral charge (from 300 to 600 ppm approximately). The generated colloid mass increases when the tetrahedral charge increases; this might depend on the fact that stronger interactions between tetrahedral layers may favour the formation of large particles which are detachable for the larger Na content.

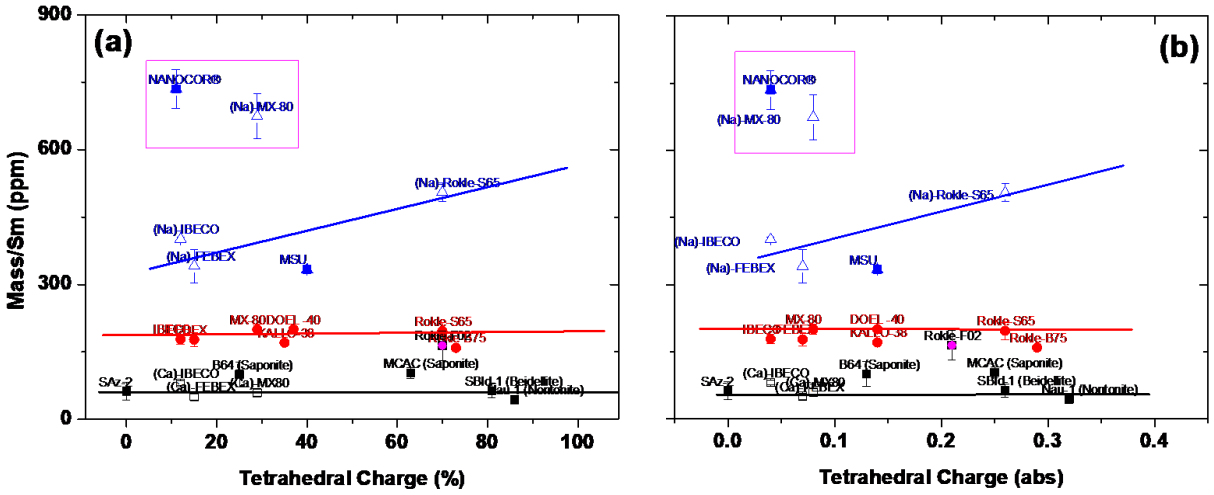

Figure 5. Mass of colloid generated normalized to the smectite content as a function of the (a) charge in the tetrahedral layer; (b) Absolute tetraedrla charge. ◢ Na Clays; △ Homoionic Na-Clays; ● (Ca,Na)-mixed Clays; ■ Ca-Clays; □ Homoionic Ca-Clays.

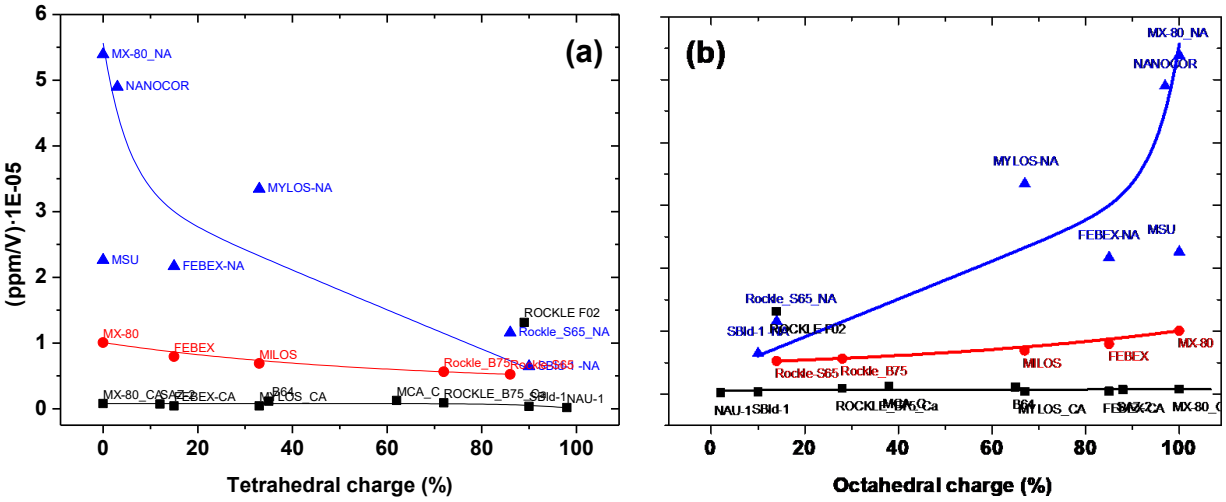

Figure 6. Relation between total mass and particle volume (ppm/V) as a function of (a) tetrahedral charge in the tetrahedral layer and (b) absolute octahedral charge. ◢ Na Clays; ● (Ca,Na)-mixed Clays; ■ Ca-Clays.

To observe the relation between the "number of released clay colloids", and the percentage of tetrahedral charge, the data were also plotted as normalised mass (ppm) divided to particle volume (Figure 6).

The number of the released particles is proportional to the ratio between the total mass and the volume of the particles.

Particle volume was calculated with equation (7) assuming, for simplicity, spherical particles:

$$V = \frac{4\pi(R_H)3}{3} \qquad (7)$$

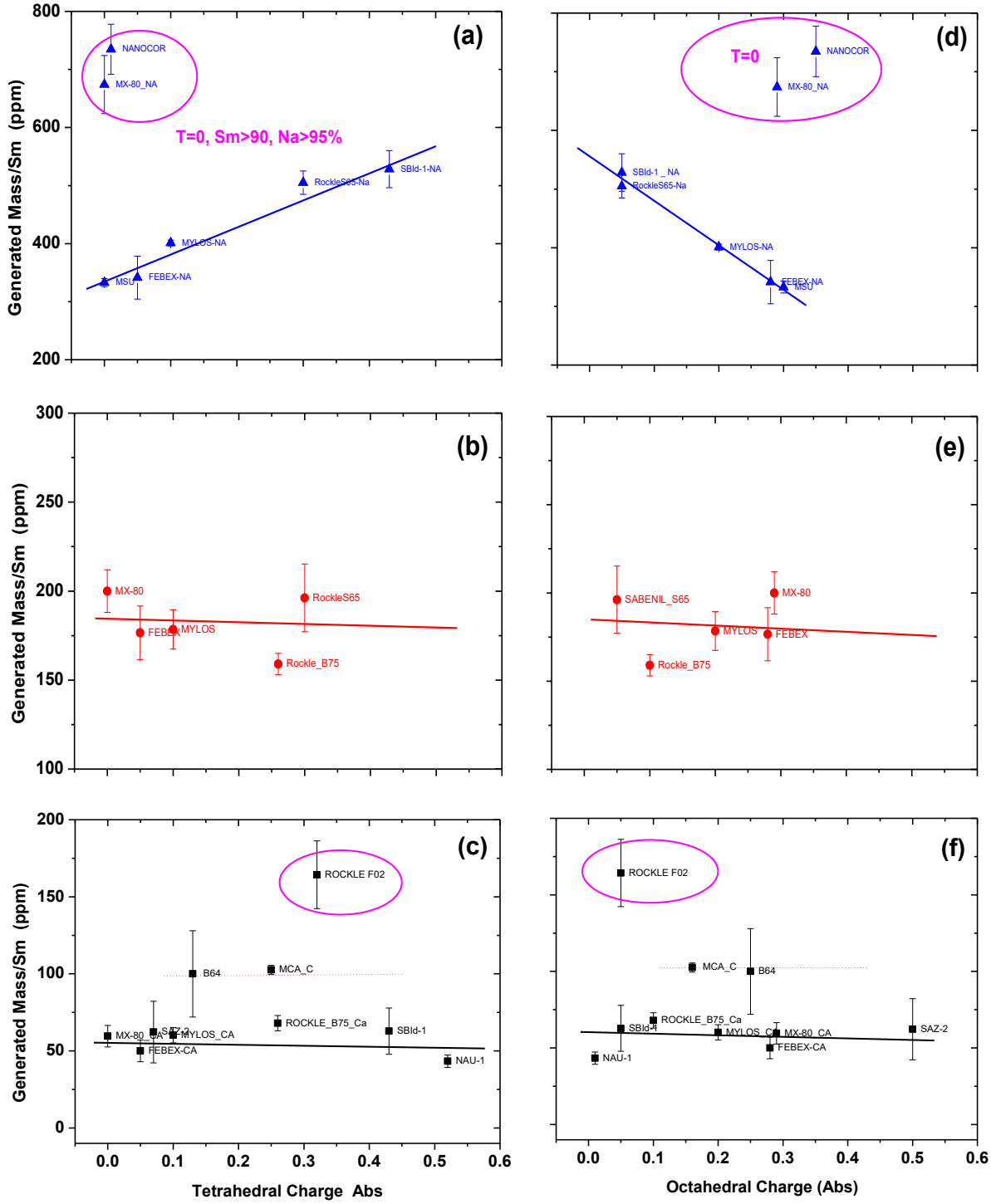

Figure 7. Mass of colloid generated normalized to the Sm content as a function of the absolute value of the tetrahedral (left) or octahedral (right) layer charge. (a-d) Na-Clays; (b-e) Na-Ca-Mixed-clays; (c-f) Ca-clays.

Data for hydrodynamic radius (R_H, in nm) were taken from measured hydrodynamic particle sizes, gathered in Table 5 and Table 6. The "number of released clay colloids" tends to decreases when the percentage of tetrahedral charge increases: this effect is present in all the cases even is much more evident for Na-clays. Considering that the "mass" of colloid generated and "number of colloidal particles" might give rise to apparently different results both will be considered for further discussion.

Figure 6b shows the data (ppm/V) as a function of the percentage of the octahedral charge. A predominance of octahedral charge give rise to the opposite effect, i.e. it makes easier particle release.

Figure 7 shows the dependence on the colloid mass generated normalised to the Sm content as a function of the absolute value of the tetrahedral charge (left) or octahedral charge (right). In the case of mixed and Ca-clays no clear dependence can be seen, the presence of Ca in enough high quantity is a predominant factor over the charge distribution.

It seems that saponites MCA-C and B64 show slightly higher values of generation than di-octahedral Ca-clays. The Rokle-F02 behaviour seems to be anomalous due to it shows the highest values of generation, which is probably due to the presence of oxides

In the case of Na clays, the highest mass is always released when T=0, Sm >90 and Na >95% as already observed. Then the mass of colloid generated increases with the absolute tetrahedral charge. This behaviour may be related to the previously discussed fact that particle size is increasing as tetrahedral charge increases. The increase of the absolute octahedral charge produces a decrease in colloid generation (again samples with T=0, Sm>90 and Na>95% are different)..

Figure 8 shows the ratio ppm/V (proportional to number of released particles) as a function of the absolute tetrahedral charge (left) or octahedral charge (right). For Ca-clays, again, the distribution of charge is not very relevant; for Na and Na-Ca mixed clays the number of particles generated decreases with increasing the tetrahedral contribution to the total charge. The opposite is true for the octahedral charge.

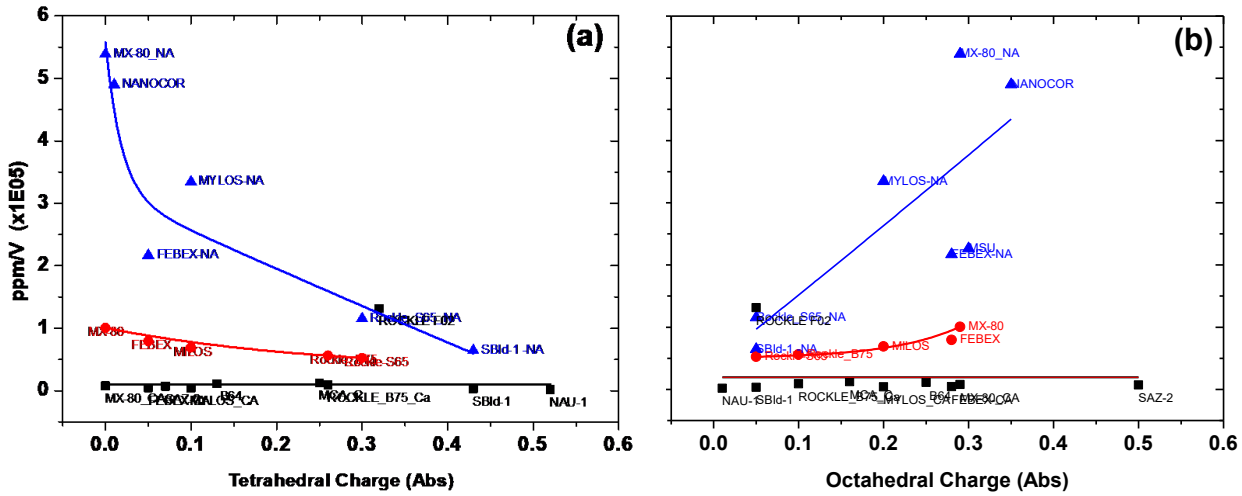

Figure 8. Relation between total mass and particle volume as a function of (a) the absolute value of tetrahedral charge and (b) the absolute value of octahedral charge.

Figure 9 shows the mass generation as a function of the charge density, which again give similar information. Figure 9a shows the mass of colloids normalized to the smectite content and Figure 9b the number of particles. Figure 8a showed that some variation is seen only in Na-clays where the

ones with T=0 behave differently, for the others the mass increases with increasing the charge density, again due to the increased size of the particles.

Figure 9b shows that the number of released particles decreases if layer charge density increases, which is expected due to a less interaction between platelets.

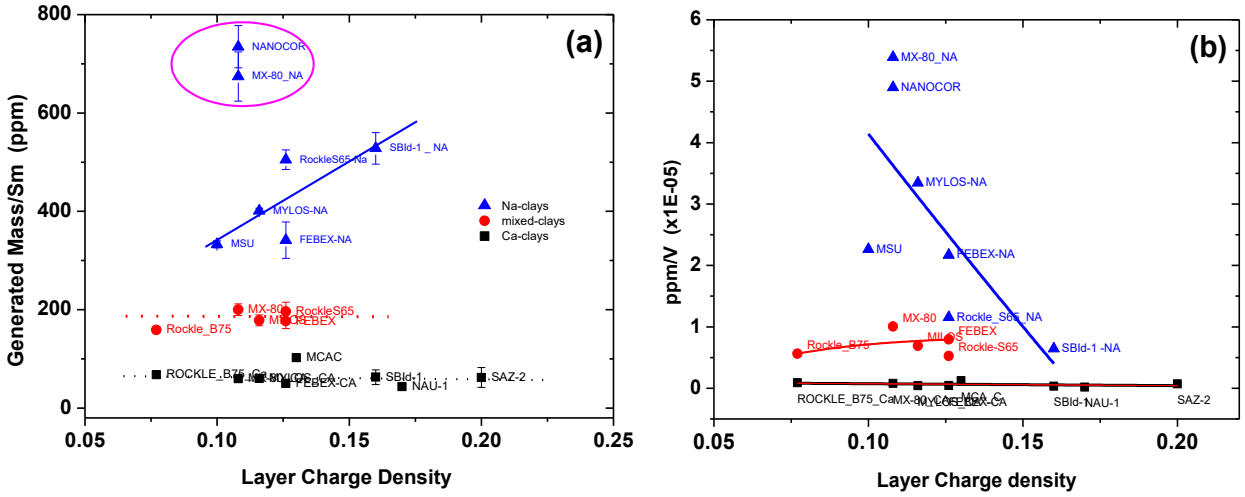

Figure 9. (a) Colloid mass normalised to the smectite content and (b) particle number as a function of the layer charge density.

Figure 10 shows the data as a function of the total layer charge. Similar information than that obtained in Figure 9 can be seen. In general, Ca-clays are subjected to interlayer forces high enough and independent on the layer charge and/or charge density. As far as the content of Ca in the system decreases, more particles can be detached the lower the layer charge/charge density the larger the number of particles. In term of mass, the highest always corresponds to the samples with T=0, Sm>90 and Na>95%. An increase of layer charge/charge density may cause an increase of the size of the particles, therefore (just) in Na-clays the mass of colloids tends to increase accordingly. In Na-clay particles can be easily detached as the strenghtness of layer interaction is weakened.

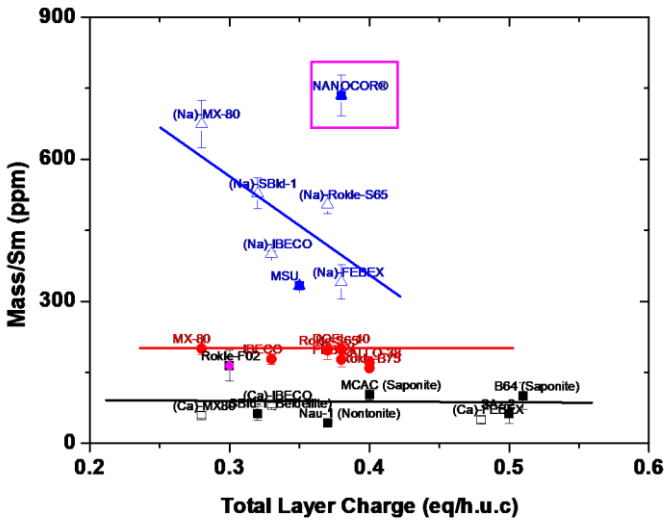

Figure 10. Relation between total mass and smectite content as a function of the total layer charge (eq/h.u.c).

3.4 ANALYSIS OF PARAMETERS AFFECTING HYDRODYNAMIC COLLOID SIZE

The mean initial size of the colloids generated by the different clays is summarised in Table 5 (as received clays) and Table 6 (exchanged clays). The size measured by photon correlation spectroscopy (PCS) is the hydrodynamic size, which includes the molecules of water adhered to the particles while they are moving. The data related to colloid size, as previously done for the colloid mass, will be related to other physicochemical properties of the clay: Na content, total layer charge and charge distribution.

3.4.1 NA CONTENT

The size of the particles is expected to depend on the Na content in the exchange complex. Figure 11 shows the variation of particle size as a function of Na (%) percentage in the exchange complex.

The highest colloid sizes (>500 nm) corresponds to Ca-clays; the difference measured in the size of Ca-clay are important, up to values of approximately 800 nm. Thus, the presence of Ca as exchangeable cation above the 80%, clearly favours the formation of large particles. The unique exception is the Rokle-F02, with a size lower than 300 nm, which also was observed to be "anomalous" also in the analysis of colloid generation. In any case, this presents (at sight) very large sedimenting flocs, thus PCS measurement might be biased.

When the Na in the exchange is above a 20% a drop in size is clearly observed. The size of mixed-clays is more or less contained within the range of approximately 350-450 nm. Most of the Na-clays have a size around 250-300 nm, except Rokle-65-Na and SBId-1-Na, which clearly shows higher sizes than Na-Ca mixed clay (*they might be not completely Na-exchanged*).

The difference in size for Na- and Ca-clay must be explained by other factors than the Na content as interlayer cation, and these factors will be analysed below. It has also to be taken into account that the size measurements for big particles are more difficult due to their rapid sedimentation.

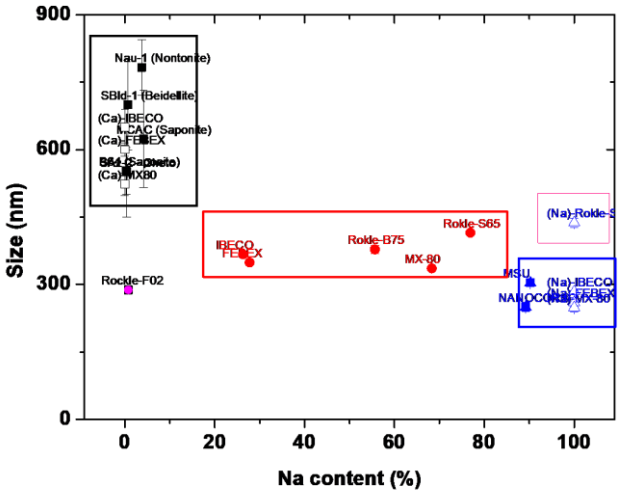

Figure 11. Particle size as a function of the Na content.

3.4.2 CHARGE AND CHARGE DISTRIBUTION

Figure 12 shows the dependence of the particle size on the distribution of charge and, in particular, on the tetrahedral charge (% of tetrahedral charge, left column; absolute tetrahedral charge right column).

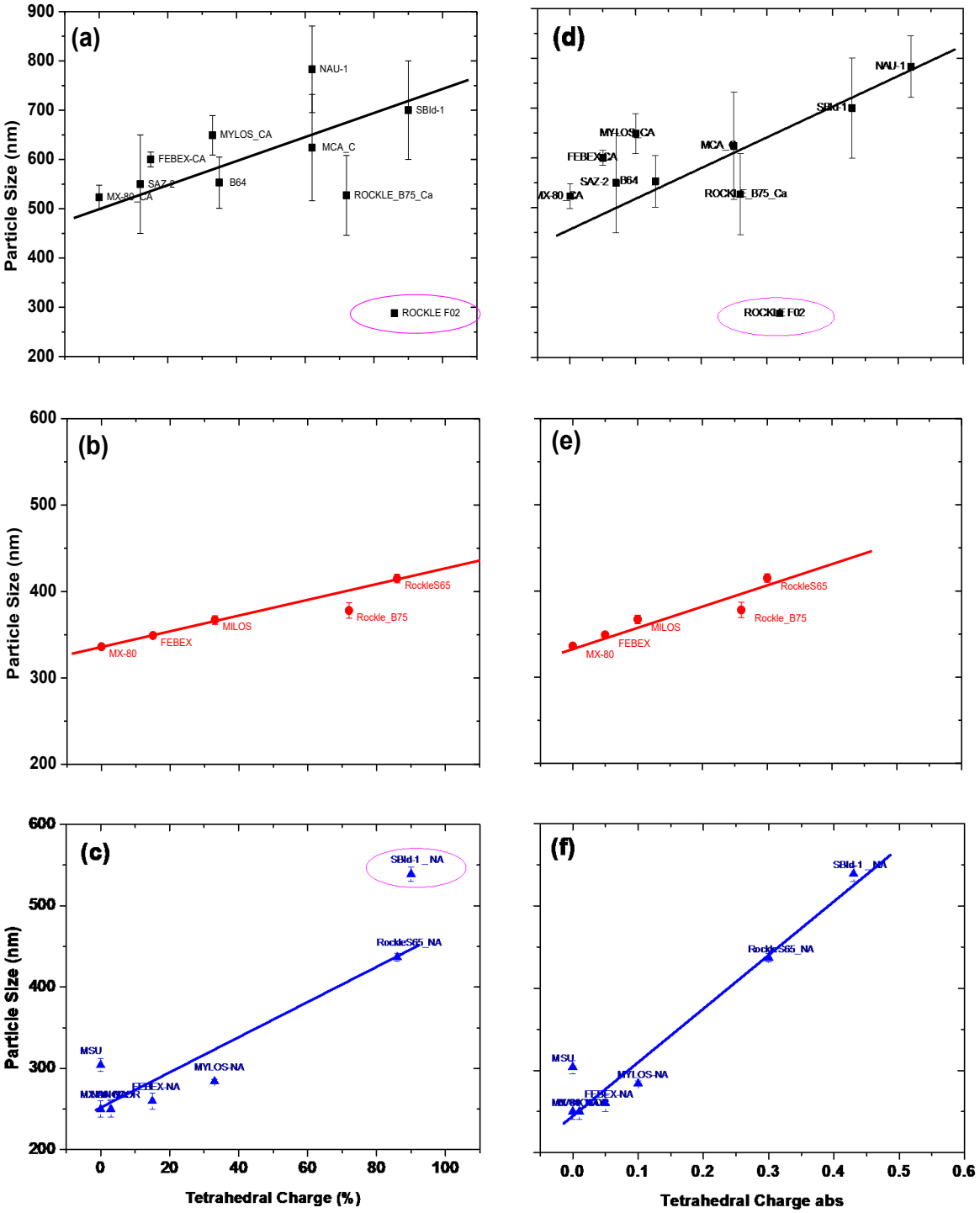

Figure 12. Particle size as a function of the tetrahedral charge substitution (left column) and absolute tetrahedral charge (right column). (a-d) Ca-Clays; (b-e) Mixed-clays; (c-f) Na-clays.

It is interesting to note that for all the types of clays, the size of the particles is progressively increasing with the tetrahedral substitution, i.e. the higher the substitution in the tetrahedral layer, the larger the particle size. This confirms the hypothesis related to the increased mass loss in Na-clays when the tetrahedral charge increases. The stronger bond between the cations and the clay layer surface promoted by the charge located in the tetrahedral layer also favours the aggregation between different particles.

The same information is obtained considering the absolute value of the tetrahedral charge (Figure 12, right figures).

This means that the lower the tetrahedral charge and the tetrahedral substitution are, the smaller particles will be formed, within the range allowed by the presence of Ca as interlayer cation.

The “apparently” too large size of the Na-Sabenil-65 and Na-SBId-1 could be then explained by the large tetrahedral charge (even if the Na-SBId-1 still shows an odd behaviour).

This nice dependence is verified in all the cases but in the case of Rokle-F02. The difference of size between Na- and mixed clays is not very large, even though the dependence with the charge distribution is clear. The tetrahedral charge seems to be the most important parameter controlling the colloid size, along with Ca content.

Similarly, if the hydrodynamic size is plotted as a function of the octahedral absolute layer charge, as shown in Figure 13, the behaviour is the opposite: size decreases with increasing the total contribution of octahedral charge. The position of the charge in the smectite is thus a fundamental parameter to be accounted for one of the most important characteristic of colloids: their size. As commented before, very large particles are subject to rapid sedimentation, thus measurements are subject to larger errors.

Figure 14 shows the particle size as a function of the charge density. In general, the tendency is the increase of the size as the charge density increases. SAz-2 and Rokle-B75 did not follow the behaviour of other clays. In the case of mixed clays, the dependence of the size on the charge density is very small.

Figure 15 shows the hydrodynamic radius of all clays as a function of the layer charge. No correlation is observed.

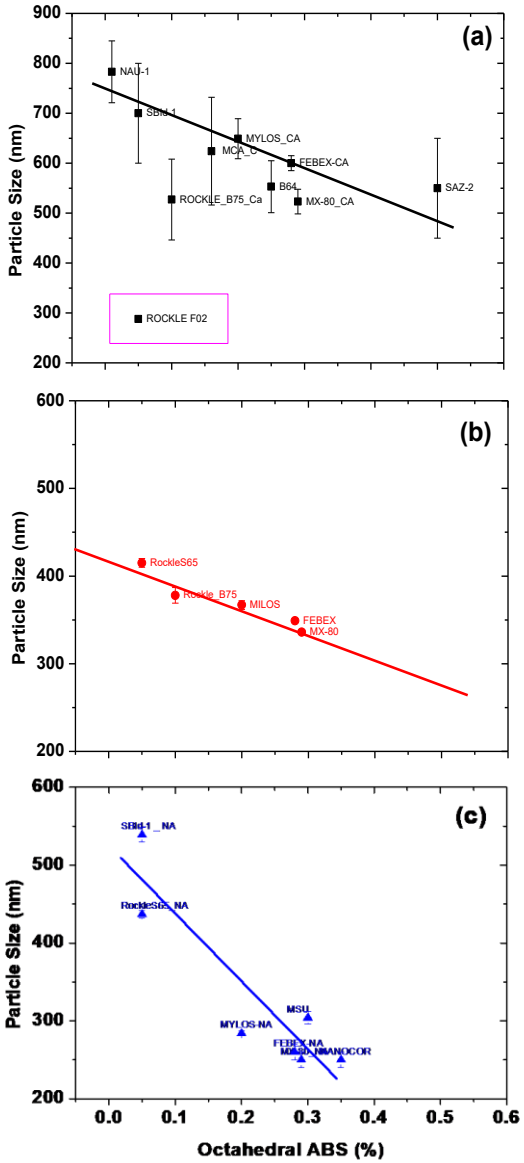

Figure 13. Particle size as a function of absolute octahedral charge a) Ca-Clays; (b) Na-Ca-Mixed-clays; (c) Na-clays.

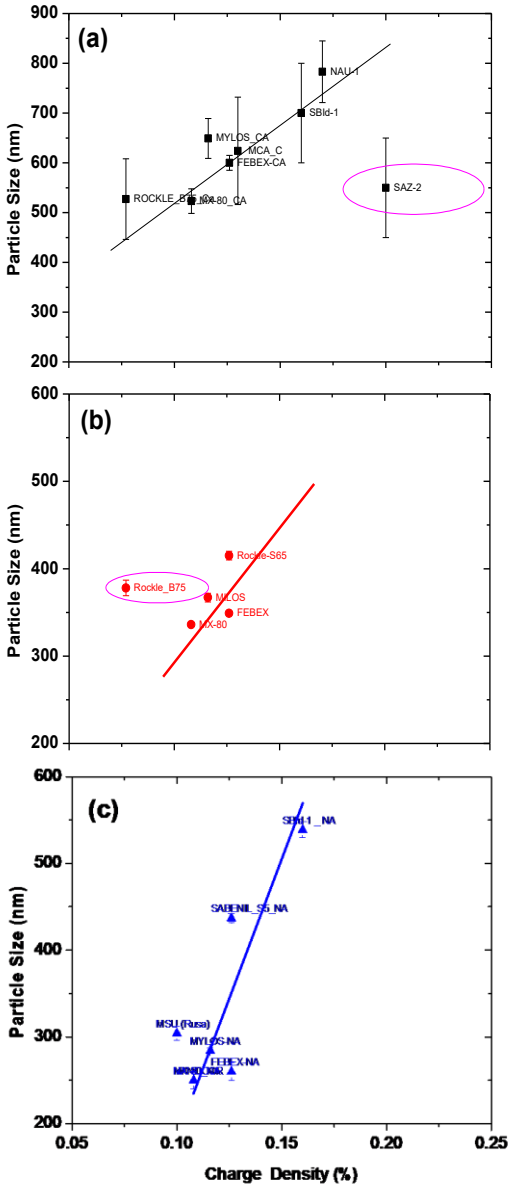

Figure 14. Particle size as a function of charge density a) Ca-Clays; (b) Na-Ca-Mixed-clays; (c) Na-clays.

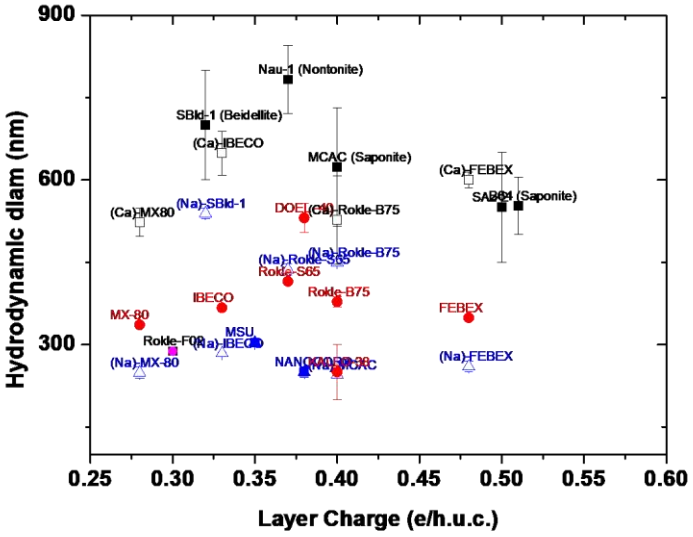

Figure 15. Particle size as a function of the layer charge.

3.4.3 SURFACE AREA (BET)

It has been reported [72] that the ratio between the external and total surface area (SA) is an indicative of the number of tactoids, which form a clay particle, thus must be related with the particle size. In order to verify this for our size measurements with PCS, the hydrodynamic diameter was plotted as a function of the SA/BET (external and total area) in Figure 16. Excluding the Rokle-F02, and Ca-clays the other clays are all well correlated.

The Rockle-F02 always presents an anomalous behaviour, probably because it presents a large quantity of (iron) oxides, which can be released as colloidal particles disguising their presence the actual behaviour of the clay colloids. Excluding the Rockle-F02 and Ca-clays, the other clays are well correlated.

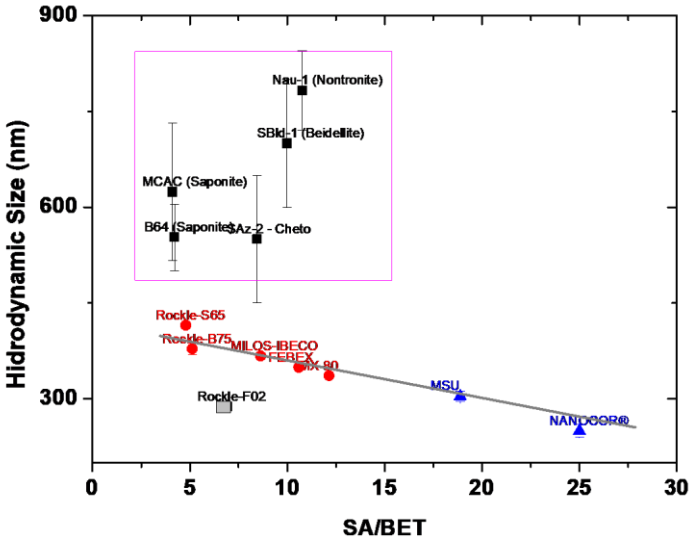

Figure 16. Particle size as a function of the SA/BET ratio.

3.5 ANALYSIS OF PARAMETERS AFFECTING COLLOID MOBILITY AND ZETAPOTENTIAL

3.5.1 NA CONTENT

The determination of colloid charge was done by means of electrophoretic mobility measurements. The mobility of colloids in the initial suspension will be related to the main properties of the clay, firstly on the main exchanging ion.

Figure 17 shows the mobility of colloids in the initial suspensions as a function of the content of Na in the exchange complex. The electrophoretic data were expressed as mobility $(\mu m \cdot s^{-1})/(V \cdot cm^{-1})$. Knowing that the clay charge is always negative, *decreases and increases* in mobility will be referred to absolute values.

The mobility of all the clays ranges from approximately -1 to -3 $(\mu m \cdot s^{-1})/(V \cdot cm^{-1})$. The mobility of 2:1 clay is negative, according to their negative permanent charge [73,74,75]. Small variation on charge are observed as a function of the pH, above all in the range of pH of the suspensions considered here (from 7 to 9; Table 3). The amphoteric charge present on the edge surface groups is much smaller than the permanent charge [73] and zetapotential values of smectites are dominated by their layer charge.

Ca-clays present smaller values of electrophoretic mobility. Amongst Ca-clays, only beidellite SBId-1, and nontronite Nau-1 show significantly higher mobility values than the others. The mobility is very sensitive to the valence of the ion adsorbed on the clay, and this fact is well known [76]: Ca-clays show less mobility, but it is observed that a 35% of Na in the exchange complex is enough to provide electrophoretic mobility similar to those of Na-clays, as observed also in this study.

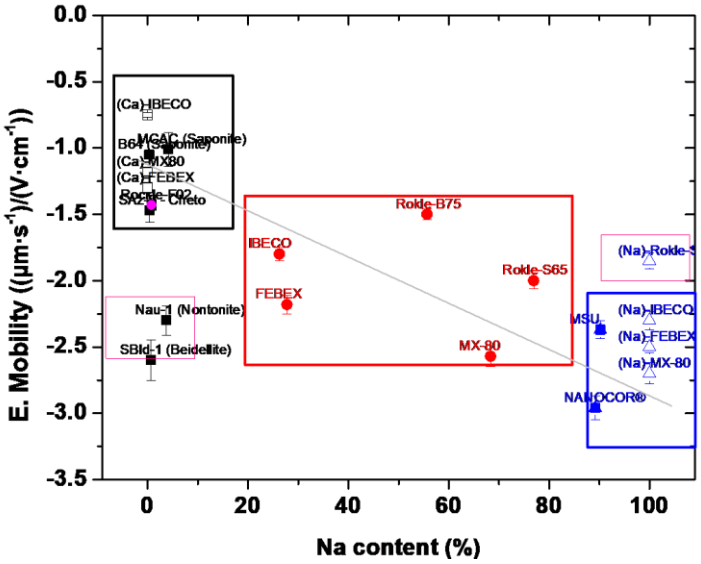

Figure 17. Electrophoretic mobility as a function of Na in the exchange complex.

3.5.2 CHARGE AND CHARGE DISTRIBUTION

The electrophoretic mobility data measured for the clays, showed considerable dispersion, even classified by principal groups, and this might be related to other properties of the clay.

Figure 18 shows the electrophoretic mobility expressed as a function of the tetrahedral charge substitution (left column) and absolute tetrahedral charge (right column).

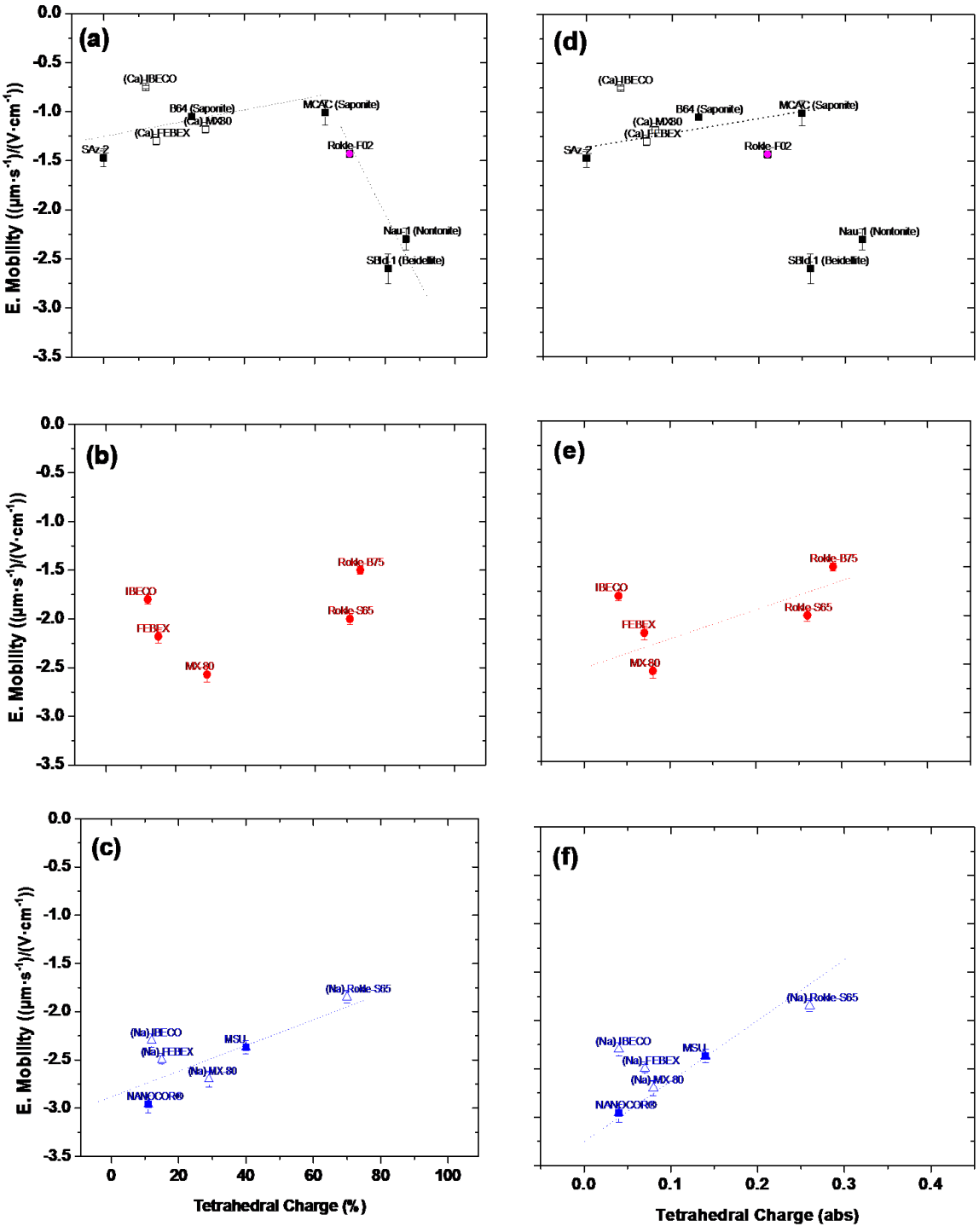

Figure 18. Electrophoretic mobility as a function of the tetrahedral charge substitution (left column) and absolute tetrahedral charge (right column). (a,d) Ca-Clays; (b,e)Mixed-clays; (c,f) Na-clays.

The position of the charge in tetrahedral sites is more accessible and localised, therefore is better neutralised by cations, for this reason it is expected that, when T is low, the apparent potential is more negative.

However, the mobility of Ca-clay varies slightly in dependence on the degree of tetrahedral substitution, even though beidellite SBId-1 and nontronite Nau-1, which presents almost null octahedral charge (Table 1), are different from the others.

This is due to the fact that Ca is a strongly binding ion and it is able to screen the permanent charge, independently on its position. When Ca in the system decrease above a 80%, a different behaviour is observed and, a clear effect of the tetrahedral charge can be seen. The anomalous samples are RokleS65 (both as received and Na exchanged), which show higher mobility than the expected according to its tetrahedral charge, and SBId-1-Na. This last sample deserves a special mention; in fact, it was very difficult to determine its mobility, because it was like a dense gel and had the tendency to progressively charge during the measurements. The final reported value might not be correct.

Thus, an increase of the tetrahedral charge provokes a decrease in the overall clay mobility but not in Ca-clays, where the effect is not appreciable.

Figure 19 shows the mobility as a function of the absolute octahedral charge. In all the cases an increment of octahedral charge produces an increment of mobility (not considering beidellite SBId-1 and nontronite Nau-1 which are anomalous in terms of mobility because they have null octahedral charge (O=0).

Figure 20 shows the plots of electrophoretic mobility as a function of the clay charge density (a) or total charge (b). Not clear effects on charge density or total charge can be seen, except perhaps for Ca-clays, where a certain increase of mobility with the charge density/layer charge is observed. Other authors [74] analysed the effects of layer charge ion the electrophoretic mobility of smectite; they found that the layer charge and the ionic strength did not largely influence the electrophoretic mobility of smectite at neutral to alkaline pH.

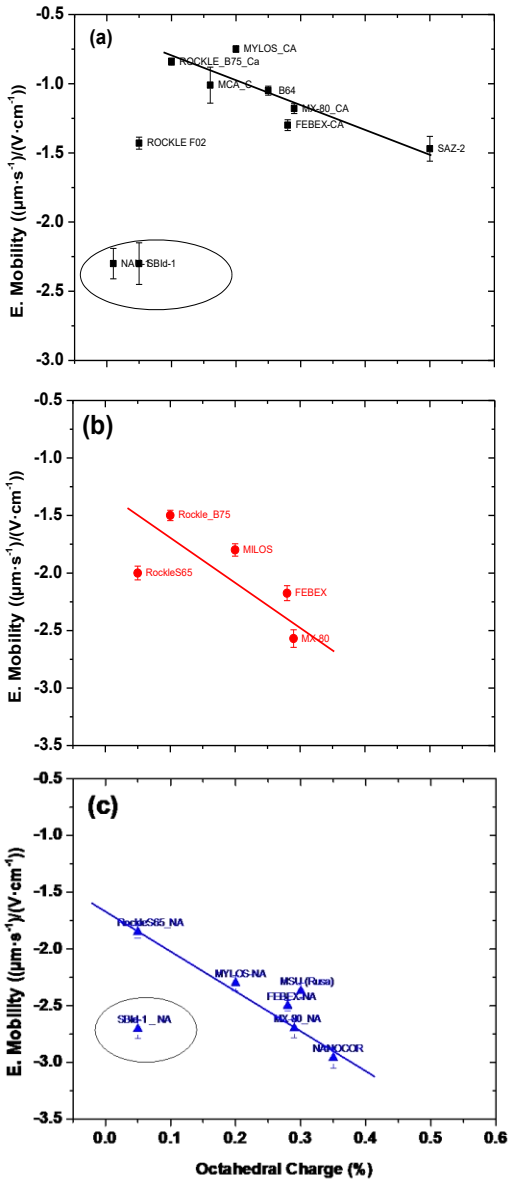

Figure 19. Electrophoretic mobility as a function of absolute octahedral charge a) Na-Clays; (b) Na-Ca-Mixed-clays; (c) Ca-clays.

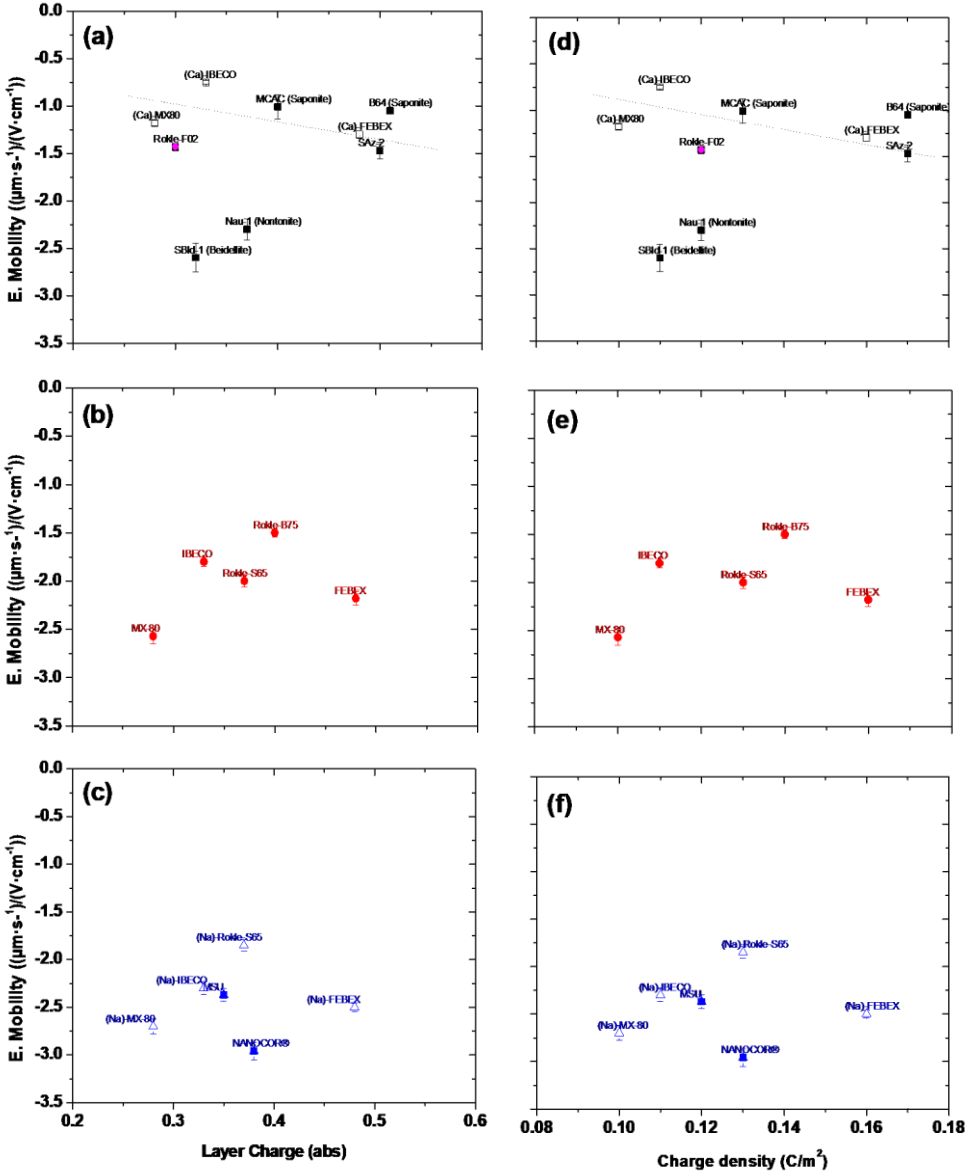

Figure 20. Electrophoretic mobility as a function of (a) charge density and (b) total charge.

3.6 REFERENCE ZETAPOTENTIAL

The zetapotential for each sample upon the addition of 1mM Na^+ has been considered as the reference zetapotential value. A reference value of the zetapotential for each clay was recalculated using the Smoluchowski approximation, at the [Na] of 1 mM. The dependence of the zetapotential on other parameters is discussed below. These zetapotential values are also collected in Table 7.

CLAY	Initial size (nm)	Onset Coag. (Na,mM)	Onset Coag. CNa,mM)	Size >1um (Na, mM)	CCC Na/Ca (approximate)	Zeta at 1mM Na (mV)
FEBEX	349±1	10-20	0.1-0.2	>30	100	-33.4±1.6
MILOS-IBECO	367±5	2-3	0.1-0.2	10-20	17	-26.2±0.9
MSU	304±8	4-5	0.1-0.2	20-30	30	-32.0±0.5
MX-80	336±2	10-20	0.2-0.3	>30	60	-35.1±1.1
NANOCOR®	306±1	10-20	0.2-0.3	>30	60	-37.7±1.1
NAu-1 (Nontonite)	783±62	10-20	0.2-0.3	10-20	60	-32.2±1.5
Rokle-B75 (Par. Act)	378±9	2-3	0.1-0.2	10-20	17	-24.5±1.8
Rokle-F02	288±4	4-5	0.1-0.2	>30	30	-27.2±0.7
Rokle-S65 (Fully Act)	415±5	1-2	0.05-0.1	5-7	20	-28.2±1.0
SAz-2 – Cheto	550±100	1-2	0.1-0.2	10-20	10	-21.3±1.7
SBId-1 (Beidellite)	700±100	2-3	0.05	3-4	50	-37.7±1.1
B64 (Saponite)	553±52	5-7.5	0.2-0.3	20-30	25	-22.5±0.4
MCAC (Saponite)	624±108	1-2	0.05	3-4	30	-25.0±1.4

Table 7. Main characteristics of the colloids generated in DW from the different clays. Raw clays.

Figure 21 shows the reference zetapotential plotted as a function of the Na content in the exchange complex. The zetapotential values are similar for all the clays (between -25 and -40 mV) with a slight tendency to increase (in absolute value) as the Na content increase, as already observed in the case of mobility values. The two Ca-clays which have an anomalous behaviour, having quite high zetapotential values, are beidellite SBId-1 and nontronite NAu-1.

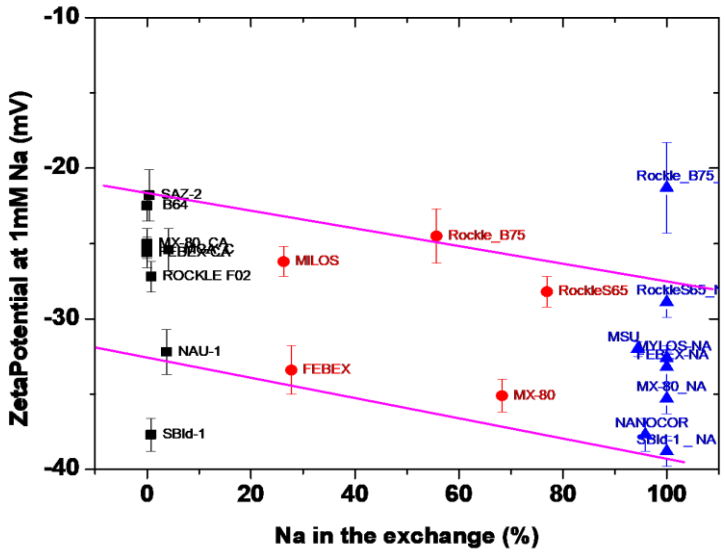

Figure 21. Zetapotential measured after the addition of 1mM Na as a function of the Na content in the exchange complex.

Figure 22 shows the reference zetapotential as a function of the tetrahedral charge substitution (left column) and absolute tetrahedral charge (right column). In Ca-clays, the zetapotential tends to slightly increase (in absolute value) as the tetrahedral substitution and absolute tetrahedral charge increases. This is not straightforward to explain.

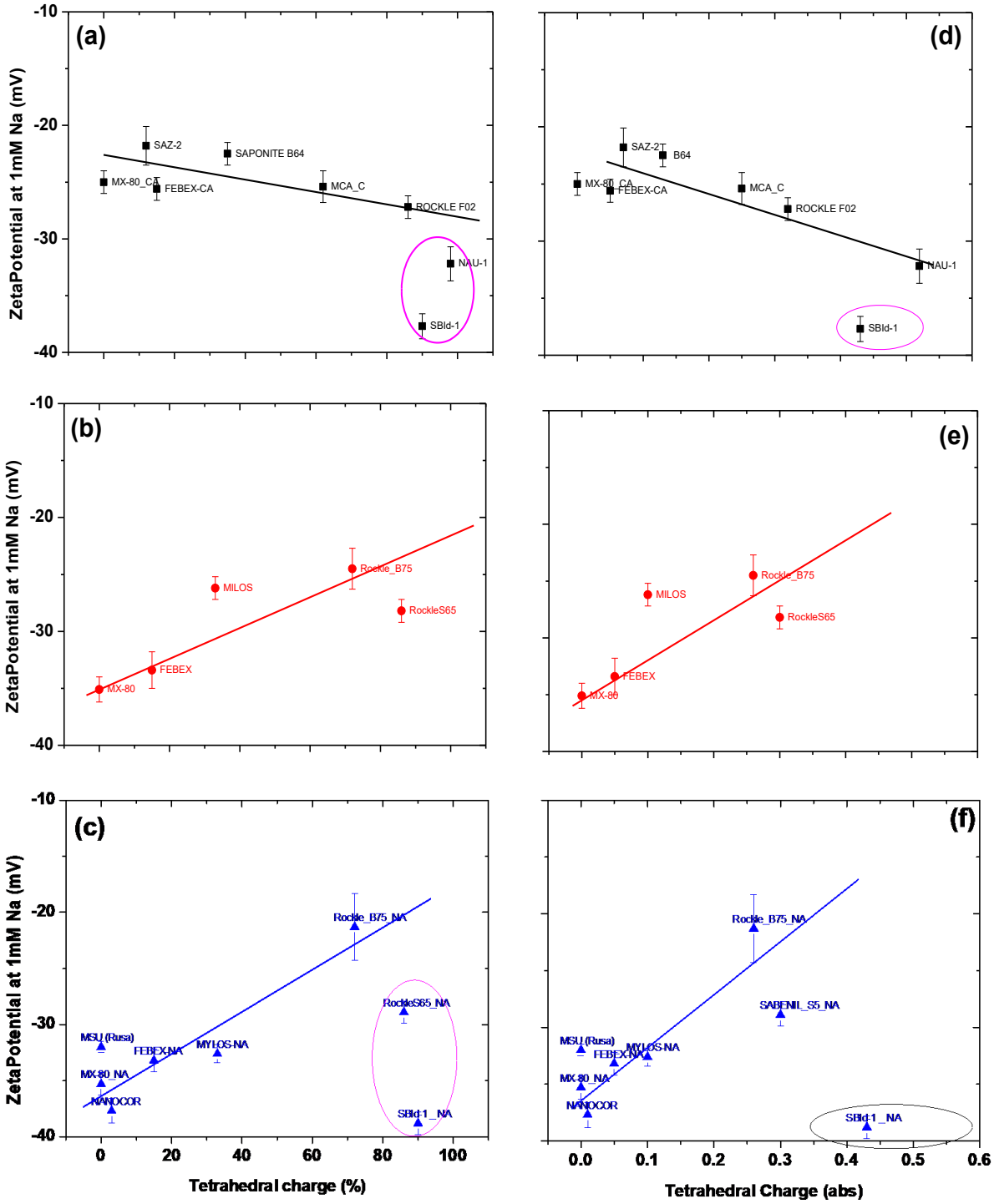

Figure 22. Zetapotential measured after the addition of 1mM Na as a function of the tetrahedral charge substitution (left column) and absolute tetrahedral charge (right column). (a,d) Ca-Clays; (b,e)Mixed-clays; (c,f) Na-clays.

In Na-Ca mixed and Na-clays, the zetapotential decreases in absolute value as the absolute tetrahedral charge and the tetrahedral substitution decreases, and basically, the same behaviour observed for mobility can be seen.

Figure 23 shows the plots of the reference zetapotential as a function of the total layer charge (Figure 23a) and charge density (Figure 23b). Not clear effects on charge density or total charge (very similar in all the cases) are observed.

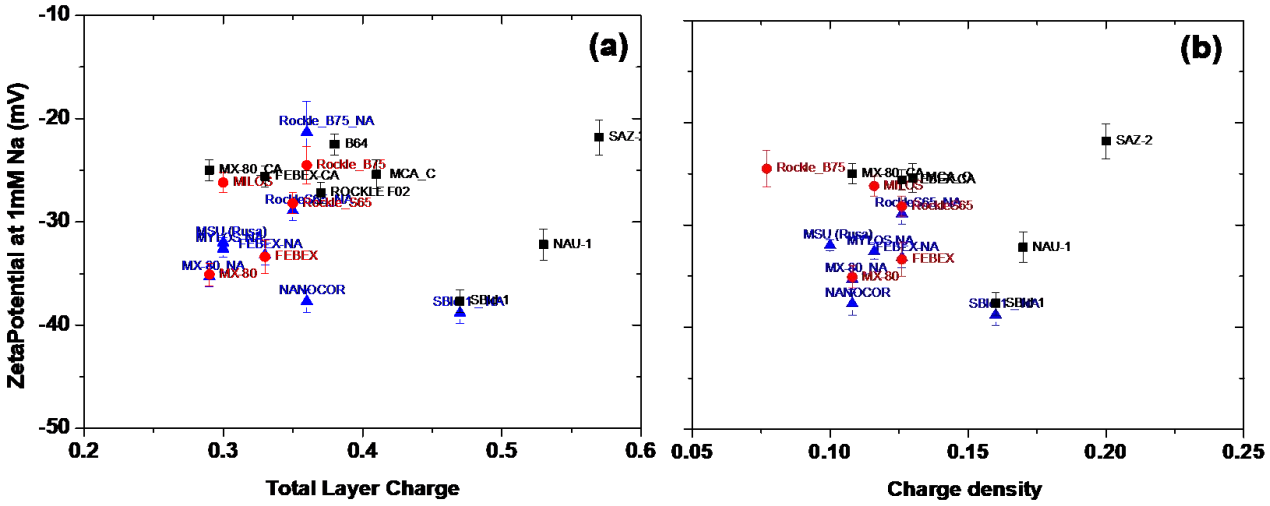

Figure 23. Reference Zetapotential as a function of the (a) charge density and (b) total layer charge.

3.7 CLAY COLLOID AGGREGATION UPON ADDITION OF NA AND CA

The colloid properties (size and mobility) of different clays after progressive additions of Na and Ca have been studied. In particular, the stability of the different clays has been evaluated considering the concentration of electrolyte needed to aggregate the colloids. The results are summarised in for Na-clays, Na-Ca mixed-clays and Ca-clays, respectively.

The onset of coagulation was taken when the initial size was incremented about a 20%. The value of Na concentration needed to bring the particle size out the colloidal range (>1µm) has been also recorded. These values are summarised for as received clays in Table 7 and in Table 8 for exchanged clays.

The aggregation of clays can occur due to the increase of ionic strength promoting the diminution of the electrostatic repulsion between the particles which mainly leads to face to face, FF, interactions. Also, changes on pH may give rise to particle aggregation (edge to face, EF, or EE interactions) as the small amphoteric charge present in the edges of clay particles might interact with the negatively charged layers. These aggregates form large structures (honeycomb –like) which rapidly tend to flocculate.

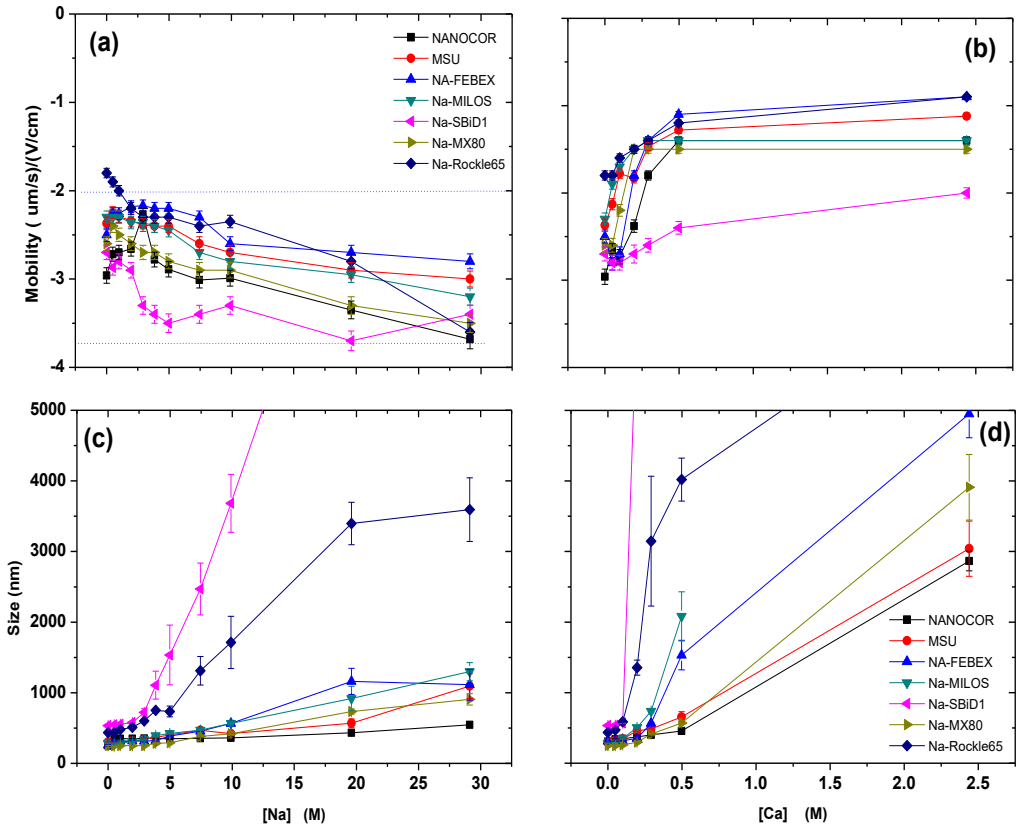

Figure 24. Variation electrophoretic mobility and particle size upon Na (a and c) or Ca (b and d) progressive additions. Na-Clays.

CLAY	Initial size (nm)	Onset Coag. (Na,mM)	Onset Coag. CNa,mM)	Size >1um (Na, mM)	CCC Na/Ca (approximate)	Zeta at 1mM Na (mV)
FEBEX-Ca	600±15	1-2	0,05	20-30	30,00	-25.6±1.0
FEBEX-Na	311±9	4-5	0.2-03	10-20	18,00	-33.2±0.8
MILOS-Na	284±3	3-4	0.05-0.1	20-30	47,00	-32.6±0.8
MX-80-Ca	523±25	10-20	0.1-0.2	>30	100,00	-28.2±1.0
MX-80-Na	288±8	5-7	0.2-03	5-7.5	25,00	-35.3±0.9
Rokle-S65-Na	437±5	2-3	0.1-0.2	5-7.5	17,00	-28.9±1.0
SBId-1-Na	539±9	2-3	0.1-0.2	10-20	17,00	-40.2±1.1

Table 8. Main characteristics of the colloids generated in DW from the different clays. Exchanged clays.

Depending on the type of aggregation, the properties of the material may change, for example FF aggregates are less viscous than EE or EF ones. However, as commented before, within the range of pH of the suspensions analysed in this study the charge from these edges is less important, thus, coagulation due to ionic strength is more important. Specific adsorption of cations, which provokes changes of the surface potential, can be also a cause of aggregation.

The electrophoretic data were expressed as mobility $(\mu m \cdot s^{-1})/(V \cdot cm^{-1})$ and decreases and increases in mobility are referred in terms of the absolute value.

Figure 24 shows the variation of mobility (Figure 24 a-b) and size (Figure 24 c-d) of Na-clays after the addition of Na or Ca. In relation to the mobility, it can be seen that when Na is added to the

system (Figure 24a) a slow progressive increase of the negative electrophoretic mobility is produced, whereas the opposite is observed when Ca is added (Figure 24b). The mobility in presence of Ca is smaller because as previously mentioned; Ca more easily neutralizes the clay charge.

The mobility of all the samples is qualitatively similar and the trend of variation is similar for all the clays within approximately two units. The mobility after Na additions ranges approximately between -2.0 and -3.8 $(\mu m \cdot s^{-1})/(V \cdot cm^{-1})$ (minimum and maximum values measured) whereas after Ca addition, the mobility ranges from -3 to -1 $(\mu m \cdot s^{-1})/(V \cdot cm^{-1})$.

The mobility measurement of the sample Na-SBId-1 presented some problems due to the charging of the sample, and this clay showed the highest mobility values. The following samples with highest electrophoretic mobility are the NANOCOR® and MX-80 clays, which are Na-clays with null tetrahedral charge. These characteristics make the adsorbed cations to have less capacity to neutralize the layer charge.

Also after Ca addition, the sample that shows the highest mobility is the Na-SBiD-1, which behaves different from the other Na-clays. Upon the addition of the electrolytes (both Na and Ca), the aggregation of the particles is observed Figure 24c-d) as expected when the ionic strength of the solution increases. Comparing Figure 24c and Figure 24d, it is clear that the aggregating power of Ca is much higher than that of Na as most of the samples are fully aggregated at Ca concentration lower than 1 mM.

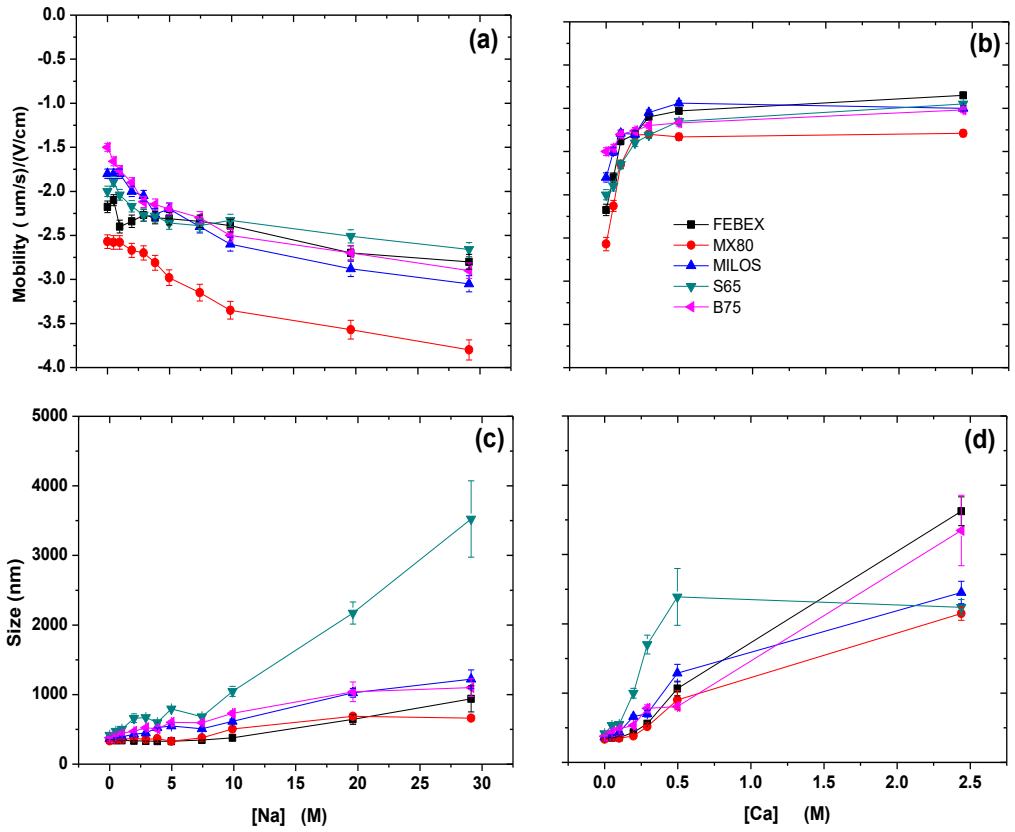

Figure 25. Variation of size and electrophoretic mobility upon Na (a and c) or Ca (b and d) progressive additions. Mixed Clays.

The samples faster aggregating are the beidellite Na-SBId-1 and the Na-Rokle65. The case of the beidellite is striking because it apparently develops the highest surface potential. The fact that this sample forms a dense gel might be the indication that it forms very large structures where, in spite of the elevated tetrahedral charge, Na is not able to compensate the layer charge.

Figure 25 and Figure 26 show the stability tests for Na-Ca mixed and Ca-clays, respectively. The general behaviour is similar to that already discussed for Na-clays. Amongst the mixed clays, the sample which develops more negative potential is the MX-80, which has almost null tetrahedral charge. The initial sizes of colloids from Ca-clays are higher with respect to those generated in Na- or Na-Ca mixed clays and even small quantities of Na, are enough to produce aggregation of particles out of the colloidal range.

The samples which are faster destabilised are: the Rokle-B65 amongst the Na-Ca mixed clays; and beidellites, saponites and nontronite amongst the Ca-Clays. In general, the onset of aggregation after adding Na varied from 1-2 mM, to 10-20 mM. Nevertheless, the onset of coagulation after adding Ca occurred with concentrations one or two orders of magnitude lower (from 0.05 to 0.3 mM). In most of the cases, the size increases above the limit of "colloid size" when 10-30 mM of Na are added. No substantial difference can be seen, for the different clay types.

The concentration of ion which produces the aggregation can be considered as the "critical coagulation concentration" (CCC) of the clay. The values found in this work are in agreement with other previously reported [77].

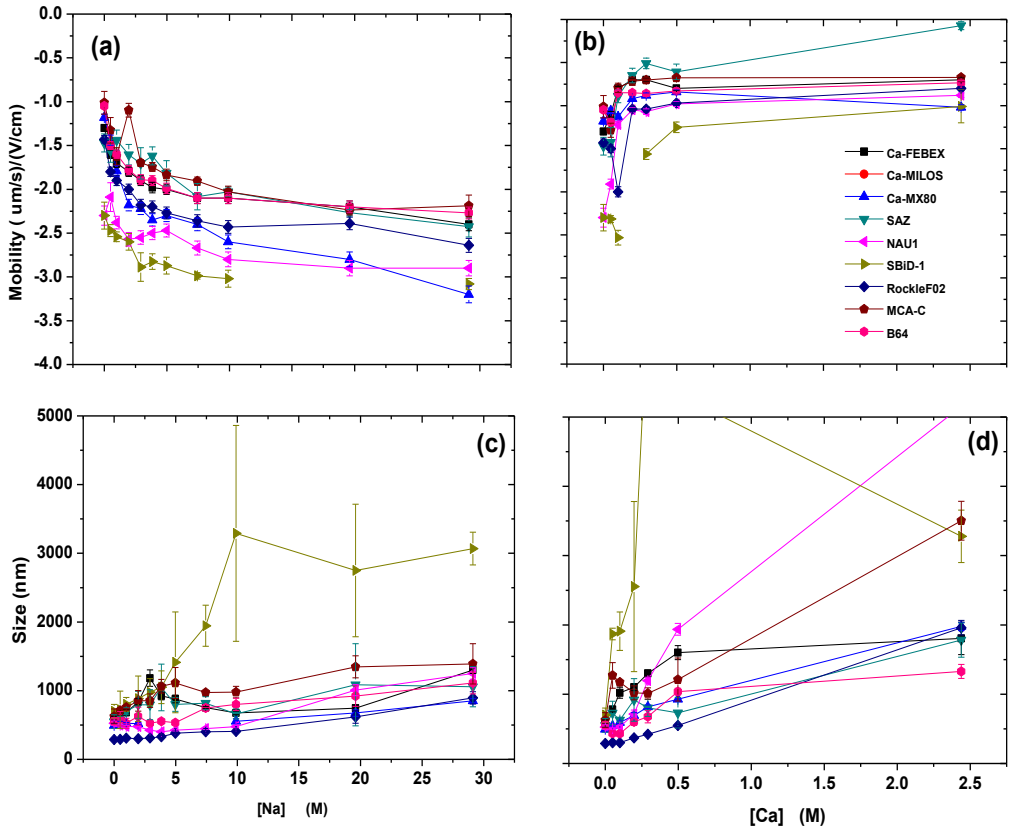

Figure 26. Variation of size and electrophoretic mobility upon Na (a and c) or Ca (b and d) progressive additions. Ca- Clays.

The aggregating power of Ca is higher than that of Na. The Shoulze-Hardy rule assumes that the CCC of an ion depends on the the sixth power of its valence (CCC ~$1/z^6$). However, the ratio between the CCC of Na and Ca, calculated from the data of the present work, is not exactly that predicted by the Shoulze-Hardy rule, varying from 10 to 100 (theoretical 64). A relation of this ratio with other properties of the clay could not be established, probably due to the experimental procedure adopted (CCC is determined within intervals not with a detailed titration; the "aggregation" is established upon a 20% increase of initial size, etc). In any case, the result it is not surprising considering that the intrinsic properties of the clays have a large effect on colloids characteristics.

It is important to point out that the observed increase of mobility, upon the increase of the Na content in the system is not in agreement with the Gouy-Chapman theory and the conventional description of the double-layer. Considering Equation 3, if the charge density is a constant (as expected in the case of 2:1 clays) the surface potential should decrease if the electrolyte concentration increases [75], as the double layer is shrinking. However, Horikawa et *al.* [78] suggested that clays must have almost constant surface potential within a large range of Na concentration and must be considered as surfaces of constant potential rather than constant charge.

The same anomalous behaviour of the clay mobility (or zetapotential) increasing the Na concentration in solution has been observed also in other studies [79,80]. Even the mobility decreases, the fact that the double layer is less repulsive increasing the Na content is demonstrated by the evident aggregation of the particles. Some authors explained this anomaly considering a charge spillover caused by layer compression, i.e. a sort of rearrangement of the electrical field around the edges. As the edges (neutral or positively charged) are screened, the net negative charge increases. This spillover occurs with Na because the double layer produced by Na ions is not as compact as that produced by divalent ions.

When Ca is added, the electrophoretic mobility decreases as predicted by the DDL theory. The DDL is enough compressed and the spillover of charge on the edges is negligible.

Results indicate that the double layer theory may not be directly applicable to explain the charge behaviour of clay particles and that other mechanisms than those described by Gouy Chapman theory must be taken into account. To assess the stability of a clayey system the parallel measurement of zetapotential and the size is always needed.

4 COMPARISON WITH EROSION BEHAVIOUR UNDER COMPACTED CONDITIONS

In the present study, the dispersion of smectite clays was analysed in deionised water, under the most favourable conditions, that can be taken as the maximum erodibility. Maximum colloid dispersion has been measured for Na-homoionic smectites, while significant lower values were dispersed from Ca-smectites. It was shown that the governing clay characteristics that promote colloid dispersion are the smectite content, the Na predominance as interlayer cation, and the layer charge and the charge distribution between the octahedral (O) and tetrahedral (τ) smectite layers.

However, bentonite erosion and colloid dispersion may be different under confined conditions because of, due to compaction; the clay interlayer space is in the nanometre scale, affecting the electrical interactions of charge layers (overlapping of electrical double layers). Moreover, the ion concentration of the porewater is in the molar range [81, 82, 83] which may significantly affect the water conditions at equilibrium, especially at high solid to liquid ratios.

The erosion behaviour of different raw bentonites, compacted at high density, was analysed in a confined system under favourable chemical conditions [22] in similar clay systems. To determine which physico-chemical factors are playing a major role in the erosion and colloid formation under compacted and confined conditions.

Figure 27 shows the experimental set-up used to quantify bentonite erosion and colloid formation from bentonite under compacted and confined conditions [84]. The selected dry density was 1.65 $g \cdot cm^{-3}$, a value in the upper range of densities considered by different national concepts of HLRW repositories [3].

In that set-up, the compacted bentonite pellet (approximately 4 to 4.5 grams, depending on clay humidity) was placed in a stainless-steel cylinder and it is sandwiched between two sintered stainless-steel filters. The filters have 20 mm diameter and 3 mm thickness, and a pore size of 100 μm, as can be appreciated in the SEM image presented in Figure 1b. A porosity of 38% was estimated from the dimensions and mass of the filter.

The cell is closed by two open Delrin grids that guarantee clay confinement but allowing the release of eroded particles through both filters (Figure 27c) being the total surface available for particle releases of 3.54 cm^2.

To promote clay erosion, the cell is immersed in 200 mL of deionised water (DW), to account for the most favourable conditions for erosion (low ionic strength and absence of bivalent cations) [12]. All experiments were carried out at room temperature and inside a glove box, under controlled atmosphere, to avoid dust contamination.

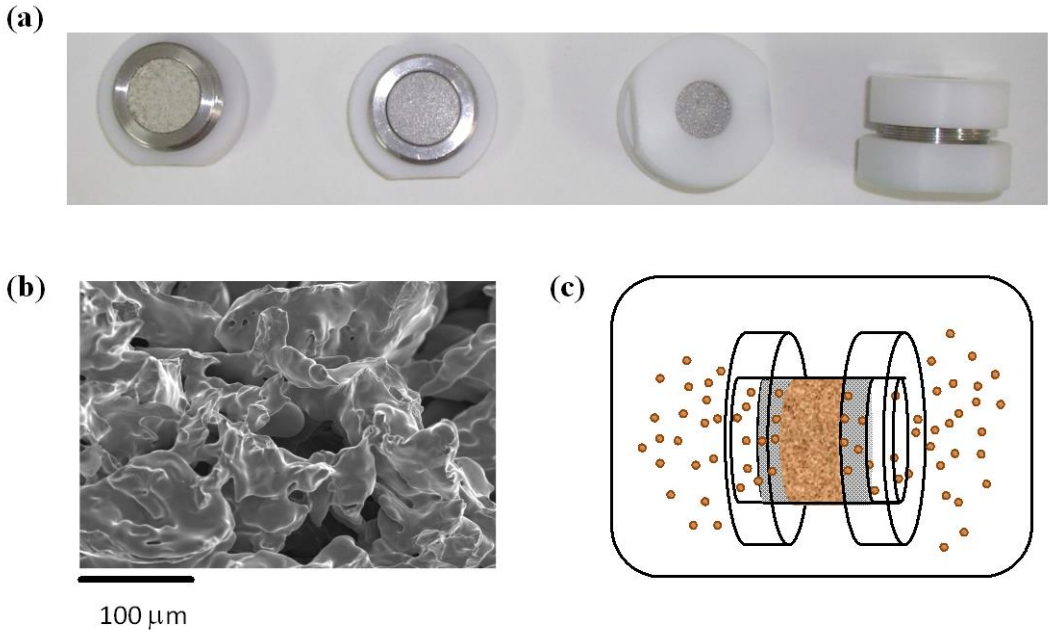

Figure 27. (a) Set-up used to analyse bentonite erosion under compacted and confined conditions; (b) SEM image of stainless steel filter surface with 100 μm pore size; (c) Outline of erosion process and colloid formation in selected set-up. [22, 71].

Erosion process in selected set-up is outlined in Figure 27C. After cell immersion in deionised water (DW), compacted clay pellet is hydrated and clay swelling is favoured but, due to confinement, free swelling is not allowed. The clay is expected to extrude through the pores of the filters, which resemble the rock micro-fractures. Eroded particles can be released to the contact water, without any additional force. By analysing the liquid phase, we measure the fraction of particles eroded and released to the liquid phase, as described in [22].

Figure 28 presents the eroded mass (in mg) measured, as a function of time, in 200 mL of electrolyte in contact to the different raw bentonites compacted at 1.65 $g \cdot cm^{-3}$ and adequately confined. The initial electrolyte is deionised water (DW). Figure 28a shows those experiments where measured eroded masses were appreciable (mass > 5 mg). The highest values are measured for FEBEX clay (40 mg), followed by MX-80, NANONOR® and MILOS-IBECO clays, which are clays with exchangeable Na+ content higher than a 20% of the cation exchange capacity (CEC) and an smectite content (Sm.) $\geq$ 80 wt.% (Table 1).

In Figure 28b, the eroded mass (mg) measured for those bentonites showing limited (mass 1-2 mg: MSU, DOEL-40 and Rokle-B75) or negligible erosion (mass < 1 mg: MCA-C, NAu-1, KALLO-38, SAz-2, B64, SB-Id1) are presented.

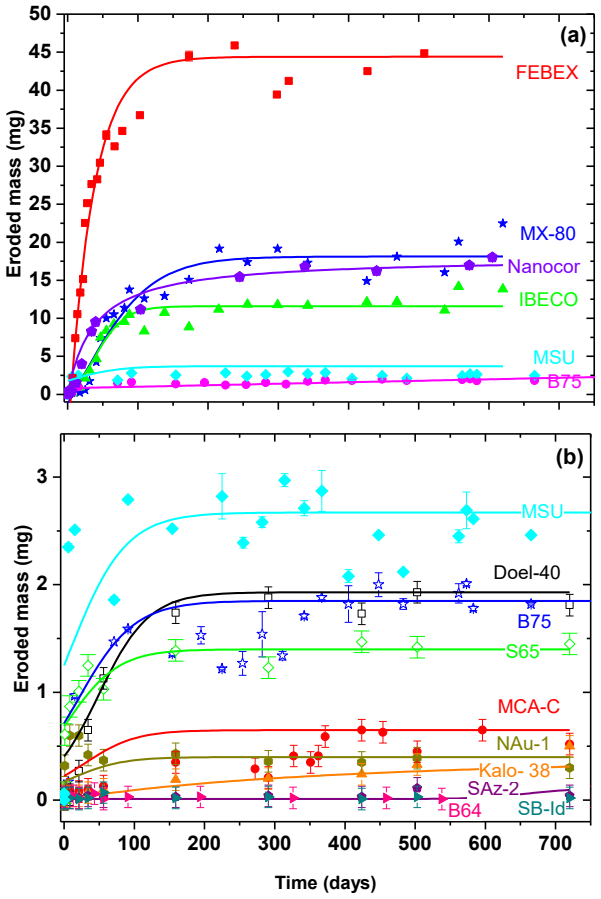

Figure 28. Eroded mass measured, as a function of time, from different raw bentonites compacted at 1.65 g·cm^{-3} and immersed in deionized water during 600-700 days. (a) Clays showing appreciable eroded masses; (b) Clays with eroded masses lower than 5 mg. The lines are included to guide the eye and the label of each clay is indicated. Data from [22].

All clays exhibited a similar behaviour in the sense that eroded mass initially increases with time but, after about 100 days, achieved an equilibrium, as previously observed [20]. However, the magnitude of erosion is significantly different amongst the different clays. Since equilibrium is reached, the average of last measured values is taken as eroded mass.

Table 9 summarizes the masses eroded (in mg) from all studied bentonites. In this table, values are presented in different units (mg and ppm) and normalised to the area available for transport (in kg·m^{-2}, considering the surface area of two filters: 3.54·10^{-4} m^2) to facilitate the comparison with other experiments.

In Table 9, the average hydrodynamic diameter measured for eroded particles is also included. It is remarkable that, when appreciable erosion was measured, the eroded particles showed an average diameter was around 300-500 nm, values that are by definition in the colloid range (< 1 µm).

CLAY	Eroded mass (mg)	Eroded mass (ppm)	Eroded mass (kg/m^2)	Size (nm)
NANOCOR®	24.8 ± 4	146 ± 24	$(7.0 \pm 1.1)\cdot10^{-2}$	248 ± 31
MSU	2.67 ±1	17.2 ± 6.4	$(7.6 \pm 2.8)\cdot10^{-3}$	299 ± 88
FEBEX	40 ± 5	268 ± 30	$(1.3 \pm 0.2)\cdot10^{-1}$	333.5 ± 42
MX-80	18.29 ± 0.5	120 ± 3.2	$(5.2 \pm 0.1)\cdot10^{-2}$	286 ± 30
MILOS-IBECO	14 ± 1	92 ± 7	$(4.0 \pm 0.3)\cdot10^{-2}$	386 ± 50
Rockle S65	1.45 ± 0.21	8 ± 1	$(4.1 \pm 0.6)\cdot10^{-3}$	468 ± 50
Rockle B75	1.9 ± 0.5	11 ± 3	$(5.4 \pm 1.4)\cdot10^{-3}$	286 ± 80
Doel-40	1.8 ± 0.1	10 ± 0.6	$(5 \pm 0.3)\cdot10^{-3}$	352 ± 22
Kallo-38	0.3 ± 0.1	1.7 ± 0.6	$(8.5 \pm 2.8)\cdot10^{-4}$	372.7 ± 71
SBDI-1 (Beidellite)	0.02 ± 0.03	0.1 ± 0.2	$(5.7 \pm 0.8)\cdot10^{-4}$	1625 ± 138
NAu-1 (Nontronite)	0.4 ± 0.22	2 ± 1	$(1.1 \pm 0.6)\cdot10^{-3}$	1260 ± 300
SAz-2 – Cheto	0.05 ± 0.04	0.3 ± 0.2	$(1.4 \pm 1.1)\cdot10^{-4}$	821.8 ± 290
MCA-C (Saponite)	0.65 ± 0.34	3.6 ± 1.9	$(1.8 \pm 0.9)\cdot10^{-3}$	995 ± 50
B64 (Saponite)	0.03 ± 0.02	0.2 ± 0.1	$(8.5 \pm 5.7)\cdot10^{-5}$	907 ± 115

Table 9. Maximum masses eroded from bentonites compacted at 1.65 $g\cdot cm^{-3}$ in deionized water, and average particle diameters measured by PCS. Eroded masses are presented in different units to consider the final water volumes (ppm) and surface available for transport ($kg\cdot m^{-2}$) calculated considering $3.54\cdot10^{-4}$ m^2 (two filters surface area). Data from [22].

4.1 SMECTITE AND NA CONTENT

Figure 29 presents the maximum masses eroded from the different raw bentonites, as a function of the smectite (Sm.) content. In this figure, the bentonites were plotted in three groups, according to their erosion, from lower to higher values: mass < 1 mg (black triangles), mass between 1 to 5 mg (red circles) and mass > 5 mg (blue squares).

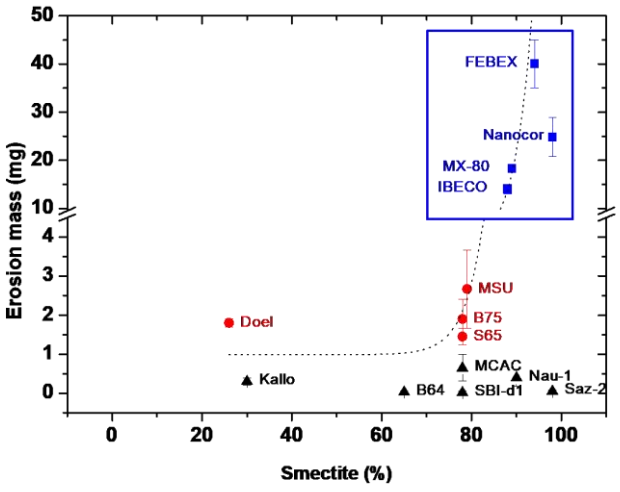

Figure 29. Eroded mass measured in deionised water from different raw bentonites compacted at 1.65 $g\cdot cm^{-3}$, as a function of the smectite content: (■) Clays with eroded mass > 5 mg, (●) Clays with eroded mass between 1- 5 mg, (▲) Clays with eroded mass < 1 mg. Data from [22].

Higher erosion is measured for clays with higher smectite content while the Ypresian clays (kallo-40, Doel-38), the with lower smectite content (Sm. < 30 wt.%), showed erosion values lower than 2 mg.

Eroded masses from clays where appreciable erosion was measured showed rather good correlation with the clay smectite content, with the exception of Nanocor ® clay, which has the highest smectite and Na^+ content (Table 1), but not the highest erosion.

In free dispersion studies, also carried out in deionised water, correlation between colloid mass released and smectite content was observed for Na- and mixed Na/Ca mixed clays (Figure 3). The dependence here is much more abrupt and erosion drops for clays with smectite content below a 90 wt.%.

Excluding Ypressian clays (DOEL-40 and KALLO-38), for their low smectite content, all smectites that showed negligible erosion (nontronite NAu-1, beidellite SBId-1, SAz-2 clay and MCA-C and B64 saponites) have very low Na content in the exchange complex (Na^+ < 10% and Ca^{2+} + Mg^{2+} > 90%); so that they can be defined as Ca/Mg clays. This indicates that high content of bivalent cations (Ca^{2+} + Mg^{2+} > 90%) is a dominant factor affecting erosion, in this case inhibiting it (Figure 3a). In fact, it is considered that sol formation does not occur in smectites with more than 90% Ca as counterions [85] been generally reported low erodibility of Ca-dominated soils [86].

The rest of the clays have smectite content from 78% (Rokle-S65 and Rokle-B75)) up to 98% (Nanocor ®) and a wide range of Na+ content: mixed Na/Ca-clays with Na+ content slightly higher than 25% (FEBEX or MILOS) up to Na-clays with Na+ content higher than a 90% of the cation exchange capacity higher than a 90% (MSU and NANOCOR ®). NANOCOR® and MSU clays have higher Na^+ content but they are not the most eroded clays, being erosion mass higher for FEBEX with a Na^+ content lower than 30%. Therefore, eroded masses are not correlated to the Na^+ content.

This independence of masses eroded from compacted clays of the clay Na content was at first sight striking, because it is well-known that the presence of Na^+ in the interlayer (approximately above 20%) causes disaggregation of clay platelets and the formation of smaller tactoids [87], and that the Na+ content in the exchange complex affects clays dispersion [88]

However, we have seen that free-dispersion experiments, higher colloid masses were generated from laboratory exchanged Na-homoionic clays (Figure 3), but similar quantity of colloids were generated from raw mixed Na/Ca clays.

The fact that masses eroded from Na-homoionic clay samples verify dependency on the Na content, not clearly observed in raw clays, suggests that accessory minerals or oxides present in the clay, the salt inventory and /or properties related to compaction are playing an important role.

One of the characteristics of compacted smectite clays is its swelling capacity, and thus, a relationship between erosion mass and swelling pressure is not discarded. Swelling ability of smectites is affected by the water uptake and their salinity, by the exchangeable cations [89] and by the charge distribution.

4.2 CHARGE AND CHARGE DISTRIBUTION

Figure 30 shows the mass eroded from the different bentonites, as a function of the clay tetrahedral charge per *half unit cell* (h.u.c), expressed in absolute values. In the figure, the clays whose low erodibility was already explained by their low smectite content (Sm. < 70 wt.%) or by cation exchange capacity dominated by divalent cations (Ca^{2+} + Mg^{2+} > 90%) are plotted with open symbols.

It is shown that, as previously observed under dispersed conditions (Figure 5) eroded mass decreases as the tetrahedral charge increases, with the only exception of SAz-2 clay, which have null tetrahedral charge but negligible erosion, explained by its Ca-nature, a dominant factor hindering erosion. All clays that suffer erosion have low tetrahedral charge (τ), between 0 and 0.1 *e*h.u.c, where *e* is the electron charge, while those clays whose tetrahedral charge is higher than 0.1 *e*h.u.c exhibited limited (MSU, S65 and B75) or negligible erosion (Ca/Mg-clays: beidellite, nontronite and saponite). The low erosion of saponites has been attributed to their tri-octahedral nature [90].

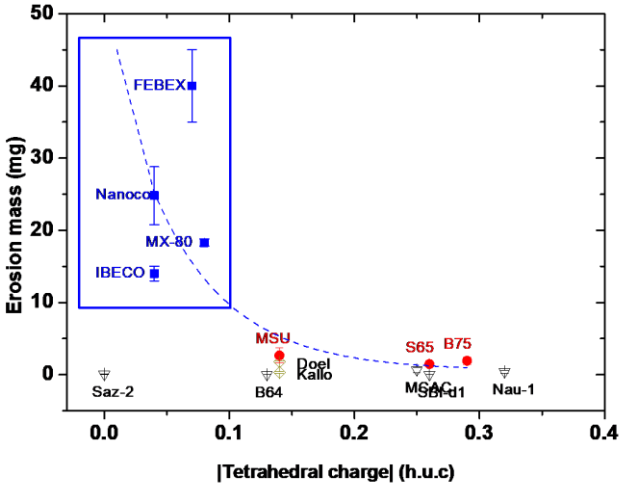

Figure 30. Mass eroded from different raw bentonites normalised to clay smectite content as a function of clay tetrahedral charge (in absolute values (e/h.u.c): (■) Clays with eroded mass > 5 mg; (●)Clays with eroded mass 1- 5 mg;. (◇) Clays with smectite content < 30% (DOEL-40 and KALLO-38); (▽) Clays with (Ca^{2+} + Mg^{2+}) > 90% (Sb-dI-1, NAu-1, SAz-2, MCA-C and B64). Data from [22].

4.3 ROLE OF ACCESSORY MINERALS

Amongst the clays that undergo erosion, eroded masses are low and actually not very different, which prevent obtaining strong dependencies. The scattering of values may be attributed to the raw nature of studied clays, which are not pure smectites, and which have accessory minerals and (oxi)hydroxides in their composition.

The erosion behaviour of clays having mixed smectite with other type of clay minerals and (oxi)hydroxides could deviate from the pure smectite behavior [91] as it has been already observed for other properties like mineralogy cation exchange [2], or swelling capacity [92]. For example, Czech bentonites (B75 and S65) have appreciable illite and kaolinite and also different Fe oxides

[51], which may contribute to inhibit erosion. The presence of certain minerals and (oxi)hydroxides affects bentonite colloid stability, and the may also affect their erosion. The ability of Al and Fe oxides to reduce clay swelling and to promote clay flocculation has been observed [93], being considered more efficient in Ca-dominated clays than on Na-clays. The relevance of minor minerals and (oxi)hydroxides present in the clay on erosion behavior should be further analysed.

4.4 ROLE OF CLAY /WATER INTERACTIONS AND CHEMICAL EQUILIBRIUM

Results showed that the low erodibility measured for most compacted clays, compared to dispersed values, can be attributed to their low smectite content, high content of divalent cations and high tetrahedral charge, but still, it is not clear why the clay with highest smectite and Na+ content, low tetrahedral charge is not the clay which exhibits highest erosion.

Under compacted and confined conditions, the solid to liquid ratio is higher than in free dispersed experiments (20 $g \cdot L^{-1}$ compared to 1 $g \cdot L^{-1}$), so that clay/water interactions may be enhanced.

The water chemistry was analysed at the end of the experiments. Table 10 presents the concentration of major ions, measured in waters in equilibrium with all studied clays, and the pH and conductivity measured at the end of the experiments. In all cases, initial water is deionised, but measured conductivities at the end of the experiment increased, indicating that dissolution of soluble salts (Table 2) present in the clay occurred.

Moreover, the concentration of cations measured (Na^+, Ca^{2+} and Mg^{2+}) in the water at equilibrium (initially deionised water) indicated that cation exchange processes took place, varying the initial content of cations in exchangeable positions. The type of dominant interlayer cation initially present is less important than the surrounding water.

According to the major anions measured, dissolution of halite (NaCl), gypsum ($CaSO_4 \cdot 2H_2O$) and also calcite ($CaCO_3$) occurred, the Cl^- and SO_4^{2-} concentrations being in agreement with the anion inventory present in the clays (Table 2). The clay with higher anion content in the salt inventory is NANOCOR®, probably coming from the industrial treatment used to homoionise the clay.

The ionic strength was calculated with measured cation and anion concentrations, and obtained values are confirmed by measured conductivities (Table 10).

Figure 31 presents the eroded mass obtained from the different bentonites as a function of the ionic strength at equilibrium. In this figure, the clays whose low erodibility was explained by their low smectite content (Sm. < 60 wt.%), by their high content of divalent cations ($Ca^{2+} + Mg^{2+} > 90\%$) and by their high tetrahedral charge ($|\tau| > 0.1$ h.u.c) are plotted with open symbols.

The ionic strength values measured for Ca/Mg clays were low while the highest ionic strength (~ 10^{-2} M) were measured for the Na-clays (NANOCOR® and MSU), values explained by soluble salts (Cl^- and SO_4^{2-}) in their inventory. The rest of the clays have values between $2 \cdot 10^{-3}$ M and $9 \cdot 10^{-3}$ M, and showed good correlation to eroded masses: the lower the ionic strength the higher the erosion.

CLAY	pH_{FIN}	$Cond_{FIN}$ mS/cm^2	Ca^{2+} (M)	Mg^{2+} (M)	Na^{+} (M)	K^{+} (M)	HCO_3^{-} (M)	SO_4^{2-} (M)	Cl^{-} (M)	Ionic strength (M)
NANOCOR®	7.42	673.00	$8.7\cdot10^{-6}$	$1.5\cdot10^{-4}$	$6.5\cdot10^{-3}$	$2.6\cdot10^{-5}$	$1.2\cdot10^{-3}$	$2.2\cdot10^{-3}$	$6.8\cdot10^{-4}$	$8.6\cdot10^{-3}$
MSU	9.88	719.00	$1.0\cdot10^{-5}$	$8.6\cdot10^{-6}$	$8.3\cdot10^{-3}$	$5.9\cdot10^{-5}$	$6.6\cdot10^{-3}$	$4.8\cdot10^{-4}$	$3.9\cdot10^{-4}$	$8.9\cdot10^{-3}$
FEBEX	8.20	190.00	$1.2\cdot10^{-5}$	$9.2\cdot10^{-5}$	$1.9\cdot10^{-3}$	$2.6\cdot10^{-5}$	$4.9\cdot10^{-4}$	$2.3\cdot10^{-4}$	$4.2\cdot10^{-4}$	$2.0\cdot10^{-3}$
MX-80	8.86	364.00	$1.4\cdot10^{-5}$	$8.6\cdot10^{-5}$	$3.7\cdot10^{-3}$	$3.3\cdot10^{-5}$	$3.0\cdot10^{-3}$	$7.0\cdot10^{-4}$	$1.0\cdot10^{-4}$	$5.1\cdot10^{-3}$
MILOS-IBECO	9.30	286.00	$1.2\cdot10^{-5}$	$4.5\cdot10^{-5}$	$2.7\cdot10^{-3}$	$3.1\cdot10^{-5}$	$2.5\cdot10^{-3}$	$2.7\cdot10^{-4}$	$3.7\cdot10^{-4}$	$3.7\cdot10^{-3}$
Rockle S65 (fully activated)	9.75	600.00	$1.5\cdot10^{-5}$	$1.3\cdot10^{-5}$	$2.6\cdot10^{-4}$	$6.7\cdot10^{-5}$	$7.8\cdot10^{-3}$	$1.5\cdot10^{-5}$	$2.6\cdot10^{-4}$	$7.4\cdot10^{-3}$
Rockle B75 (part. activated)	9.32	393.00	$1.9\cdot10^{-5}$	$2.3\cdot10^{-5}$	$5.2\cdot10^{-3}$	$1.5\cdot10^{-4}$	$1.6\cdot10^{-3}$	$4.0\cdot10^{-5}$	$1.7\cdot10^{-4}$	$3.9\cdot10^{-3}$
Doel-40	9.20	437.00	$3.5\cdot10^{-5}$	$1.4\cdot10^{-5}$	$4.0\cdot10^{-3}$	$2.1\cdot10^{-4}$	$4.8\cdot10^{-3}$	$1.4\cdot10^{-4}$	$1.0\cdot10^{-3}$	$5.9\cdot10^{-3}$
Kallo-38	8.64	395.00	$1.3\cdot10^{-5}$	$8.6\cdot10^{-6}$	$3.6\cdot10^{-3}$	$1.7\cdot10^{-4}$	$3.6\cdot10^{-3}$	$2.7\cdot10^{-4}$	$3.4\cdot10^{-4}$	$4.5\cdot10^{-3}$
SBDI-1 (beidellite)	5.00	42.00	$1.6\cdot10^{-5}$	$1.1\cdot10^{-5}$	$5.2\cdot10^{-5}$	$7.9\cdot10^{-5}$	$1.6\cdot10^{-3}$	$9.2\cdot10^{-6}$	$1.1\cdot10^{-4}$	$2.6\cdot10^{-4}$
NAu-1 (nontronite)	5.63	154.00	$6.7\cdot10^{-5}$	$4.5\cdot10^{-5}$	$9.6\cdot10^{-4}$	$6.4\cdot10^{-5}$	$2.6\cdot10^{-4}$	$2.2\cdot10^{-5}$	$7.1\cdot10^{-4}$	$1.1\cdot10^{-3}$
SAz-2 – Cheto	5.87	35.00	$5.2\cdot10^{-5}$	$1.2\cdot10^{-5}$	$6.1\cdot10^{-5}$	$2.1\cdot10^{-5}$	$3.9\cdot10^{-4}$	$2.0\cdot10^{-6}$	$1.1\cdot10^{-5}$	$2.3\cdot10^{-4}$
MCA-C (saponite)	7.84	79.00	$1.9\cdot10^{-5}$	-	$3.2\cdot10^{-4}$	-	$1.6\cdot10^{-3}$	$1.9\cdot10^{-5}$	$3.2\cdot10^{-4}$	$1.2\cdot10^{-3}$
B64 (saponite)	8.11	97.00	$1.4\cdot10^{-5}$	$3.2\cdot10^{-4}$	$3.9\cdot10^{-5}$	$2.3\cdot10^{-5}$	$1.8\cdot10^{-3}$	$6.2\cdot10^{-6}$	$3.0\cdot10^{-4}$	$2.0\cdot10^{-3}$

Table 10. Chemical characteristics of water equilibrated with clay erosion cells during 600 to 700 days. Data from [22].

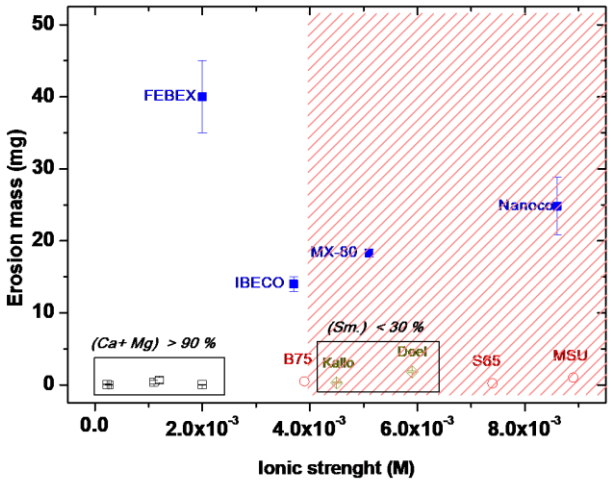

Figure 31. Eroded mass measured in deionised water from different raw bentonites compacted at 1.65 g·cm-3, in relation to the ionic strength of the contact water at equilibrium. (■) Clays with eroded mass > 5 mg; (◇) Clays with smectite content < 30% (YC-Doel40 and YC-Kallo38); (▽) Clays with (Ca+ Mg) > 90% (SB-dI-1, NAu-1, SAz-2, MCA-C and B64). (○) Clays with tetrahedral charge $|\tau| < 0.1$ h.u.c). Data from [22].

5 IMPLICATIONS FOR A HLRW REPOSITORY

The selection of the clay as engineered barrier for a high-level radioactive (HLRW) waste repository must consider several properties to guarantee its safety at the long term. The erosion of the barrier, due to chemical of physical agents, must be minimised; thus, the knowledge of the chemistry of the water, the physic-chemistry of the barrier and water rock interactions is a fundamental issue to ensure that.

The formation of the gel from the surface of the bentonite is the first step that can produce erosion. The gel must extrude in fractures, which may present fracture fillings materials that can interact with the gel.

Clay erosion is expected to have a relation with its capacity to spontaneusly disperse in water thus, the dispersability of clay is the first parameter to be accounted for. Colloid generation free-dispersion tests in DW showed that Na-clays (Na>90%, Sm>90%) are those that can may be able to disperse the highest quantity of particles (up to 80% of the initial clay mass) especially when the tetrahedral charge is (almost) null. In Na-clays an increase of mass generated is observed also when the tetrahedral charge approaches 100%, due to the increase of the particle size. Therefore, to minimise the mass loss, clays should not contain more than 80% of Na in the exchange complex; furthermore if Na content is (relatively high) high, the clay mineral should have low (but preferably not zero) tetrahedral charge.

The presence of Ca in the interlayer, in a quantity high enough (>20%), prevent clay particles from dispersion, therefore it is an important point to consider because it seems to be the most important factor (in respect to charge distribution or charge density) for erosion. Only the erosion of dispersable clays (with high Na content), seems to be affected by the charge location.

The importance of analysing the possible role of clay colloids on radionuclide migration stems on their capability of moving as fast as, or even faster, than groundwater therefore, contaminants adsorbed onto their surface might suffer faster transport [94,95,96,97,98].

The release and transport of bentonite colloids in fractures has been analysed in the past [99,100,101,102,103] and in most of the cases, their unretarded migration has been proven, even if filtration of a large part of their mass has been also observed, especially in the case of large residence times. Important aspects for colloid-driven contaminant migration are: colloid velocity in the fracture, their deposition/filtration during transport (colloid–rock interactions) and colloid stability (colloid–colloid interactions), which depends on colloid characteristics and chemistry of the medium.

For radionuclide transport the released particle must be smaller than the rock fracture aperture and colloids should be able to be transported [104].Fundamental processes controlling migration and deposition on a fracture surface are Brownian diffusion and sedimentation which are basically depending on the particle size [105 106,107] in a complex way.

Brownian diffusion is very important for small particles and sedimentation is a process favored in the case of larger particles or particles with higher density. Larger particles may suffer higher exclusion and then smaller retardation factors (Rf) [107] but higher probability of sedimentation.

In this study, it has been observed that Na-clays generally produced colloids with the smaller sizes and Ca-clays those with the larger ones, whereas the raw (mixed) clays always show very similar sizes. The main parameter affecting the colloid size was the charge distribution: an increase in the tetrahedral charge always produce an increase in size independently on the main exchanging cation.

For what concerns the stability of clay colloids, it was observed that the aggregation of the different clays under the addition of electrolytes was similar in all the cases, the aggregating power of Ca being significantly higher than that of Na, as expected, but not exactly following the Shulze-Hardy rule. The presence of particles of size larger than 1 μm, will favor sedimentation, interaction with the surface of fractures and immobilization.

Under compacted and confined conditions [22] the masses eroded were in all cases lower than those obtained under free-dispersed conditions, indicating that compacted and confined conditions were limiting for erosion. In the best situation, measured erosion was below a 1% of the initial mass.

Results clearly showed that clay erosion under compacted state is hindered for those bentonites with high content of bivalent cations in exchangeable positions ((Ca+ Na) > 90%), low smectite content (Sm. < 70 wt.%) and high tetrahedral charge ($|\tau|$ > 0.1 e/h.u.c.). In addition, it was demonstrated that, at high solid to liquid ratios, dissolution of salts present in the clay and cation exchange reactions play major role restricting erosion.

In a HLRW repository, geochemical evolution of bentonite is expected at the long term due to the water income [108] and heating [109]. Clay/water interactions and chemical equilibrium will determine erosion behaviour of a priori erodible clays over their initial physico-chemical and structural characteristics.

6 SUMMARY AND CONCLUSIONS

The colloidal fraction of the different clays was obtained suspending the 1 gr·L^{-1} of solid in deionized water (DW) and collecting the supernatant after centrifuging. The quantity of colloids present in the supernatant provided the first indication of the clay capability of dispersing colloidal particles under very favourable chemical conditions.

The mass of colloids obtained and their main characteristics (size and charge) were analysed and related to the main physicochemical properties of the clay (smectite content, main exchangeable cation, layer charge, distribution of charge between the tetrahedral and octahedral layer).

The mass of colloids generated, determined by gravimetry, was observed to depend on the smectite content for Na- and Na-Ca mixed-clays. The higher the smectite (Sm) content the higher the mass generated. This dependence was not clearly observed for Ca-clays, even though a better comparison of data could be made normalizing the mass data to the Sm content.

One of the most important parameters affecting the colloid generation was the Na content in the exchange complex, the presence of Na above 80% highly favouring colloid detachment. Quantitatively, considering that the initial clay mass was 1000 ppm, Na-clays generated from 350 to almost 800 ppm, mixed clays from 150 to 250 ppm and Ca-clays from 40 to 120 ppm of colloid mass.

However, whereas the colloid mass generated from Na-Ca mixed clays was very similar for all the mixed clays (20<Na<80); larger spread on colloid masses were observed in exchanged clays, indicating that other factors apart from the Na/Ca content are responsible of higher/lower colloid detachment to solution.

The effects of layer charge distribution on colloid formation has been therefore analysed. The colloid generation from Ca-clays and mixed was not largely affected by the distribution of the layer charge. Nevertheless, in Na-clays, the highest mass of colloids generated was observed for with almost null tetrahedral charge (NANOCOR® and Na-MX-80). Thus, under conditions favourable for colloid detachment (high Na content), very low tetrahedral charge further favours the dispersion of colloidal particles. A significant decrease of the tetrahedral charge is expected to decrease the interactions between the TOT units, favouring colloid detachment, when Ca is scarce. However, rarely, a further increase of the tetrahedral substitution, leads to an increased mass of colloids generated for Na-clays. This can be explained considering the increased size of the particles due to the increase of tetrahedral charge as the number of particles generated actually decreased. The number of released particles decreased also when layer charge density or total layer charge increased.

The size of colloid generated was determined by photon correlation spectrometry. It was also dependent on the main exchanging ions. The presence of Ca 80% leads to the formation of particles larger than 500 nm. When the quantity of Na increases above a 20% a clear drop in the particle size is observed, in agreement with the capability of Na of breaking down clay tactoids. No large difference in size are seen between Na- and mixed clays (200-300 nm). However, for all the types of

clays, the size of the particles is progressively increasing with the tetrahedral substitution, i.e. the higher the substitution in the tetrahedral layer, the larger the particle size. The stronger bond between the cations and the clay layer surface promoted by the tetrahedral charge favours the aggregation between platelets. The tetrahedral charge is the most important parameter controlling colloid size.

The surface charge of clay colloids was determined by electrophoretic mobility measurements. The mobility of clay colloids is always negative due to the negative permanent charge; in the range of pH of these suspensions, the effect of edge amphoteric charge is small. In general, the Ca-clays present less (negative) values of mobility, except some cases (beidellite SBId-1 and nontronite NAu-1) probably because divalent cations screens better than monovalent ones the negative surface charge, however the difference in the absolute values are not very large. Again, the spread in mobility data for clay with similar Ca- Na- content must be explained by other factors.

If Ca- is the main exchanging ion, no differences on mobility depending on the position of the charge are observed. The content in Ca is probably enough to screen effectively the charge independently on the type of charge (tetrahedral, octahedral). In the case of mixed and Na-clays, the mobility was observed to depend on the position of the charge. If the charge is predominantly located in the tetrahedral layer, the mobility tends to decrease. The location of the charge in tetrahedral sites is more accessible and constrained, therefore is better neutralised by cations, for this reason when T=0, the mobility is more negative.

Stability tests were carried out performing small progressive additions of Na^{+} or Ca^{2+} and measuring the variation of mean colloid size and of the electrophoretic potential. In this way, also the concentration of monovalent or divalent cation needed to start coagulation process in the different clays could be also determined. It has been shown that clay colloid aggregation is triggered by the presence of Na (10 mM) or Ca (0.1-0.2 mM) in solution indicating that they will not be stable with higher concentration of these ions.

The mobility of clay colloids slightly decreased progressively adding Na to the suspension. The fact that the double layer was less repulsive when Na was added to the system was demonstrated by the evident aggregation of the particles. However, this decrease is not in agreement with the Gouy-Chapman for a constant density of charge (as expected in the case of 2:1 clays) a decrease of the surface potential with the increase of the electrolyte concentration. The double layer theory may not be directly applicable to explain the charge behaviour of clay particles and other mechanisms must be probably considered.

The erodibility results determined under free dispersion was compared to that evaluated under compacted and confined conditions, in deionised water, to account for favourable chemical conditions for erosion. The eroded masses, measured under compacted and confined conditions and subjected to favourable chemical conditions (low ionic strength water in absence of divalent cations: deionised water), were in all cases very low. In the best situation, eroded mass measured corresponds to a 1% of the initial mass installed, by far lower than those obtained under free-

dispersed conditions, indicating that processes related to the compacted and confined conditions were limiting erosion.

Negligible erosion was measured from Ca/Mg-clays (Ca^{2+}+Mg^{2+} > 90%), independently of their smectite content or charge distribution, indicating that high content of bivalent cations in exchangeable positions is a dominant aspect affecting smectite erosion, in this case inhibiting it.

All clays which showed appreciable erosion have smectite content higher than a 70 wt.%. In addition, all erodible clays have tetrahedral charge lower than 0.1 h.u.c (in absolute value). Eroded masses decreased as tetrahedral charge (in absolute value) increases, because of clay layers interactions are strengthen, limiting detachment. However, eroded masses were not straightforward related to the main exchangeable cation, in contrast to that observed under free dispersed conditions.

The chemical analyses carried out at equilibrium partially explained the limited erosion measured under compacted conditions, in comparison free dispersed conditions. This pointed out that, under repository conditions, where solid to liquid ratio is high, the clays salt inventory and clay/water interactions may play a more relevant role on erosion than the structural characteristics of the clays.

7. REFERENCES

[1] Güven N., Bentonites – Clays for Molecular Engineering, Elements Vol 5, 89-92 (2009).

[2] Meunier A. Clays, Springer-Verlag Berlin Heidelberg, ISBN 3-540-21667-7 (2005).

[3] Sellin P., Leupin O. The use of clay as an engineered barrier in radioactive waste management – a review. Clays and Clay Minerals, 61, 477–498 (2014).

[4] Chapman, N., 2006. Geological disposal of radioactive wastes - concept, status and trends. Journal of Iberian Geology. 32, 7-14.

[5] Kaufhold S., Dohrmann R., Distinguishing between more and less suitable bentonites for storage of high-level radioactive waste, Clay Minerals, 51, 289–302 (2016)

[6] R. Pusch, Clays and Nuclear Waste Management, Handbook of Clay Science, Edited by F. Bergaya, B.K.G. Theng and G. Lagaly Developments in Clay Science, Vol. 1 pag 703-716 (2006)

[7] Dohrmann R., Kaufhold S., Lundqvist B., The role of clays for safe storage of nuclear waste. in: Handbook of Clay Science: Techniques and Applications pp. 677–710 (F. Bergaya and G. Lagaly, editors). Developments in Clay Science, Vol. 5B, Elsevier, Amsterdam (2013).

[8] Sellin P., Leupin O. The use of clay as an engineered barrier in radioactive waste management – a review. Clays and Clay Minerals, 61, 477–498 (2014).

[9] Chapman N., Hooper A., The disposal of radioactive wastes underground, Proc. Geol. Assoc. 123 (2012) 46–63.

[10] Sellin P., Nyström C., Bailey L., Missana T., Schäfer T., Červinka R., Koskinen K. BELBaR: Bentonite Erosion: Effects on the Long-term Performance of the Engineered Barrier and Radionuclide Transport Euradwaste 2013 Proceedings. EUR 26846EN Doi: 10.2777/96355 (2013).

[11] Missana T., Alonso U., Turrero M.J., Generation and stability of bentonite colloids at the bentonite/ granite interface of a deep geological radioactive waste repository. Journal of Contaminant Hydrology, 61, 17–31 (2003).

[12] Missana T., Alonso U, Albarran N., García-Gutierrez M., Cormenzana J.L. Analysis of colloids erosion from the bentonite barrier of a high level radioactive waste repository and implications in safety assessment Physics and Chemistry of the Earth, Volume 36, Issue 17, p. 1607-1615 (2011).

[13] Moreno L., Liu L., Neretnieks I., Erosion of sodium bentonite by flow and colloid diffusion, Physics and Chemistry of the Earth 36 1600–1606 (2011)

[14] Liu L., Moreno L., Neretnieks I., A Dynamic Force Balance Model for Colloidal Expansion and its DLVO-Based Application Langmuir, , 25 (2), pp 679–687 DOI: 10.1021/la8026573 (2009).

[15] Neretnieks I., Moreno L, Liu L., Mechanisms and models for bentonite erosion, TR-09-35, SKB (2009).

[16] Schäfer Th., Huber F., Seher H., Missana T., Alonso U., Kumke M., Eidner S., Claret F., Enzmann F., Nanoparticles and their influence on radionuclide mobility in deep geological formations. Applied Geochemistry, 27(2), 390-403, doi: 10.1016/j.apgeochem.2011.09.009 (2011)

[17] Pusch R. Clay colloid formation and release from MX-80 buffer. SKB Technical Report No: TR-99-31, Stockholm (1999).

[18] Birgersson M., Börgesson L., Hedström M., Karnland O., Nilsson U. Bentonite erosion. SKB technical report, TR 09-34, (2009)

[19] Svoboda J. The experimental study of bentonite swelling into fissures. Clay Minerals, 48, 383–389 (2013).

[20] Albarran N., Degueldre C., Missana T., Alonso U., García-Gutiérrez M., López T., Size distribution análisis of colloid generated from compacted bentonite in low ionic strenght aqueous solutions. Applied Clay Science, 95, 284-293 DOI: 10.1016/j.clay.2014.04.025. (2014).

[21] Pusch R, Stablity of bentonite gels in crystalline rocks: physical aspects, SKB Technical report 83-04 (1983).

[22] Alonso U, Missana T, Fernandez A M, García-Gutiérrez M, 2018. Erosion behaviour of raw bentonites under compacted and confined conditions: relevance of smectite content and chemical equilibrium. Applied Geochemistry 94, 11–20 (2018).

[23] Bergaya, F., Lagaly, G., 2013. Handbook of Clay Science. Developments in Clay Science, Vol. 5A. Elsevier, 813 pp.

[24] Sun L., Ling C.H, Lavikainen L., Hirvi J., Kasa S., Pakkanen T., Influence of layer charge and charge location on the swelling pressure of dioctahedral smectites Chemical Physics 473 (2016) 40–45

[25] Mermut A.R., Lagaly A., Baseline studies of the clay minerals society source clays: layer-charge determination and characteristics of those minerals containing 2:1 layers, Clays and Clay Minerals, 49(5), 393-397 (2001).

[26] Christidis G.E. Validity of the structural formula method for layer charge determination of smectites: A re-evaluation of published data Applied Clay Science 42 1–7 (2008)

[27] Tombacz E., Szkeres M., Colloidal behaviour of aqueous montmorillonite suspensions: the specific role of pH in the presence of mayor electrolytes. Applied Clay Science 27 75-94 (2004).

[28] Güven, N., 1988. Smectites. In: Hydrous phyllosilicates (exclusive of micas). Rev. Mineral 19, pp 497-559.

[29] Tombacz E., Szkeres M., Colloidal behaviour of aqueous montmorillonite suspensions: the specific role of pH in the presence of mayor electrolytes. Applied Clay Science 27 75-94 (2004).

[30] Petit S., Righi D., Madejova J., Decarreau A., Layer charge estimation of smectite using infrared spectroscopy. Clay Minerals 33, 579-591 (1998).

[31] Hetzel F. and Doner H.E., Some colloidal properties of beidellite: comparison with low and high charge montmorillonites, Clay and Clay minerals. 41(4), 453-460 (1993)

[32] Chrisidis G.E., Blum A.E., Eberl D.D., Influence of layer charge and charge distribution of smectite on flow behaviour and swelling of bentonites. Applied Clay Science 34, 125-138 (2006).

[33] Farmer, V.C., 1978. Water on particle surfaces. In: The Chemistry of Soil Constituens, D. J. Greenland, M.H.B., Hayers, eds. Wiley, New York, pp. 405-448.

[34] Sposito G., Skipper N.T., Sutton R., S-H. Park, A.K. Soper, J.A. Greathouse, Surface geochemistry of the clay minerals, Proc. Natl Acad Sci USA 1999, 96(7) 3358-3364 (1999).

[35] Sun L., Ling C.H, Lavikainen L., Hirvi J., Kasa S., Pakkanen T., Influence of layer charge and charge location on the swelling pressure of dioctahedral smectites Chemical Physics 473 (2016) 40–45

[36] Mermut A.R., Lagaly A., Baseline studies of the clay minerals society source clays: layer-charge determination and characteristics of those minerals containing 2:1 layers, Clays and Clay Minerals, 49(5), 393-397 (2001).

[37] Christidis G.E. Validity of the structural formula method for layer charge determination of smectites: A re-evaluation of published data Applied Clay Science 42 1–7 (2008)

[38] Leam W.F., The nature of cation-substitution sites in phyllosilicates, Clays and Clay Minerals, Vol. 38, No. 5, 527-536, 1990.

[39] cf. McBride, 1989 McBride, M.B., Chemistry of Soil Minerals. In: Minerals in Soil Environments. Dixon, J.B., Weed, S.B. (Eds.). SSSA Book Series 1, 1989, pp. 35-88.

[40] Shainberg I. and Otoh H., Size and shape of montmorillonite particles saturated with Ca/Na ions, Israel Journal of chemistry 251-259 (1968)

[41] Banin A.and Lahav N., Particle size and optical properties of montmorillonite in suspensión, Israel Journal of Chemistry, 6, 235-250 (1968)

[42] Shainberg I.and Kaiserman A., Kinetics of the formation and breakdown of Ca-montmorillonite particles, Soil Sci. Soc. Amer. Proc. Vol 33 547-551 (1969)

[43] W.R. Whalley, C.E. Mullins Effect of saturation catión on tactoid size distribution in bentonite suspensions Caly Minerals 26, 11-17 (1991)

[44] Kaufhold S. and Dohrmann R., Detachement of colloidal particles from bentonite in water, Applied Clay Science 39 50-59 (2008).

[45] Alonso U, Missana T, Fernandez A M, García-Gutiérrez M, 2018. Erosion behaviour of raw bentonites under compacted and confined conditions: relevance of smectite content and chemical equilibrium. Applied Geochemistry 94, 11–20 (2018).

[46] Miller, W.M., Alexander, W.R., Chapman, N.A., McKinley, I.G., Smellie, J.A.T., 2000. Geological disposal of radioactive wastes and natural analogues. Waste Management Series, vol. 2, Pergamon, Amsterdam.

[47] Schaefer, T., F. Huber, H. Seher, T. Missana, U. Alonso, M. Kumke, S. Eidner, F. Claret, and F. Enzmann. 2012. Nanoparticles and their influence on radionuclide mobility in deep geological formations. Applied Geochemistry 27:390-403.

[48] Missana, T., Alonso, U., García-Gutiérrez, M, Mingarro, M., 2008a. Role of bentonite colloids on europium and plutonium migration in a granite fracture. Applied Geochemistry. 23, 1484-1497.

[49] Möri, A., Alexander, W.R., Geckeis, H., Hauser, W., Schäfer, T., Eikenberg, J., Fierz, T., Degueldre, C., Missana, T., 2003. The colloid and radionuclide retardation experiment at the Grimsel Test. Site: influence of bentonite colloids on radionuclide migration in fractured rock. Colloids and Surfaces A: Physicochem. Eng. Aspects. 217, 33-47 (2003).

[50] Huertas, F. et al. Full scale engineered barriers experiment for a deep geological repository for high-level radioactive waste in crystalline host rock, EUR 19147, (2000).

[51] Fernandez, A.M. Mineralogical, Geochemical and pore water characterization of different bentonites. CIEMAT Report June 2013, 40 pp. Madrid (Spain), (2013). Fernandez, A.M. Characterization of different bentonites analysed in the context of the Belbar project. CIEMAT Report December 2017, 60 pp. Madrid (Spain), (2017).

[52] A.M. Fernández, B. Baeyens, M. Bradbury, P. Rivas – Analysis of porewater chemical composition of a Spanish compacted bentonite used in engineered barrier. Physics and Chemistry of the Earth 29 105-118 (2004).

[53] Koch, D., European Bentonites as alternatives to MX-80, Science & Technology Series 334 23-30 (2008).

[54] Müller-Vonmoss, M, Kahr, G. Mineralogische Untersuchungen von Wyoming Bentonite MX-80 und Montigel. NTB 83-13, Nagra, Wettingen, Switzerland, (1983).

[55] Konta, J. Textural variation and composition of bentonite derived from basaltic ash. Clays and Clay Minerals 34 257-265 (1986).

[56] Sabodina, M.N, et al. Behavior of Cs, Np(V), Pu(IV), and U(VI) in Pore Water of Bentonite, Radiochemistry 48 488 (2006).

[57] Post J.L, Cupp I.D.L., Madsen T., Beidellite and associated clays from the DeLamar Mine and Florida mountains área, Idaho, Clays and Clay Minerals, VoL 45, No. 2, 240-250 (1997).

[58] Keeling J.L., Raven M.D., Gates W.P., Geology and characterisation of two hydrothermal nontronites from weathered metamorphic rocks at the Uley graphite mine, South Australia, Clays and Clay Minerals, VoL 48. No. 5, 537 548 (2000).

[59] Jaynes W.F., Bigham J. M., Charge reduction, octahedral charge and litium retention in heated Li-saturated smectite, Clays and Clay Minerals, Vol. 35, No. 6, 440-448 (1987).

[60] Kastridis, I.D., Kacandes, G.H., Mposkos, E., 2003. The palygorskite and Mg-Fe smectite clay deposits of the Ventzia basin, western Macedonia, Greece. Mineral Explotation and Sustainable development, Eliopoulus et al. (eds). Millpress, Rotterdam, pp. 891-894.

[61] Stephan Kaufhold ,George D. Chryssikos , George Kacandes , Vassilis Gionis ,Kristian Ufer, Reiner Dohrmann . Geochemical and mineralogical characterization of smectites from the Ventzia basin, western Macedonia, Greece. Clay Minerals , Volume 54 , Issue 1 (2019) pp. 95 – 107.

[62] Cuevas, J., Pelayo, M., Rivas, P., Leguey, S., 1993. Characterization of Mg-clays from the Neogene of the Madrid Basin and their potential as backfilling and sealing material in high level radioactive waste disposal. Applied Clay Science, 7, 383-406.

[63] ONDRAF/NIRAS, 2001. ONDRAF/NIRAS, Technical Overview of the SAFIR2 report, ONDRAF/NIRAS report NIROND 2001-05E

[64] Nguyen, X.P., Cui, Y.J., Tanga, A.M., Li, X.L., Wouters, L.,. Physical and microstructural impacts on the hydro-mechanical behavior of Ypresian clays. Appl. Clay Sci. 102, 172–185 (2014).

[65] Dohrmann R., Kaufhold S.. Three new, quick CEC methods for determinining the amounts of exchangeable calcium cations in calcareous clays. Clays and Clay Minerals, 57(3), 338–352 (2009).

[66] Karnland and Birgersson 2006. Technical Report TR-06-30 Mineralogy and sealing properties of various bentonites and smectite-rich clay materials Ola Karnland, Siv Olsson, Ulf Nilsson Clay Technology AB.

[67] Delgado A.V., González-Caballero F., Hunter R.J., Koopal L.K., J. Lyklema, Measurement and interpretation of electrokinetic phenomena, Journal of Colloid and Interface Science 309 194-224 (2007).

[68] Horcas I., Fernández R., Gómez-Rodriguez M., Colchero J., Gómez-Herrero J. Baro A.M., WSXM: a software for scanning probe microscopy and a tool for nanotechnology, Review of Scientific Instruments, 78, 013705 (2007).

[69] Missana T., Evaluation of experimental results on bentonite erosion Deliverables D2.11 BELBAR Project 13 pp. (2016)

[70] Schatz T., Eriksson R., Hansen E., Hedström M., Missana T., Alonso U., Mayordomo N.,. Fernández A.M, Bouby M., Heck S., Geyer F., Schäfer T., WP2 partners final report on bentonite erosion Deliverable D2.11 BELBAR Project 13 pp (2016)

[71] Alonso U, Missana T., Fernandez A. M., García- Gutiérrez M., López-Torrubia T., Morejón J., Mingarro M., Sellin P, Characterrisation of different bentonites to asses their erosion behavior. Euradwaste 2013 Proceedings. EUR 26846EN. Doi: 10.2777/96355 (2013).

[72] Leonard R.A. Low P.F., Effects of gelation on the properties of clay/water systems TWELFTH NATIONAL CONFERENCE ON CLAYS AND CLAY" MINERALS Journal Paper 2243

[73] Sondi I., Biscan J., Pravdic V., Electrokinetics of pure clay minerals revisited, Journal of colloids and interface science, 178, 514-522 (1996).

[74] Thomas F., Michot L.J., Vantelon D., Monatrgés E., Prelot B., Cruchadet M., Delon J.F., Layer charge and electrophoretic mobility of smectites, Colloid and Surfaces A, 159 351-358 (1999).

[75] Luckam P.F., Rossi S., The coloidal and rehological properties of bentonite suspensions. Advances in Colloid and interface Science, 82 43-92 (1999).

[76] Bar-On P. and Shainberg I., Electrophoretic mobility of montmorillonite particles saturated with Na/Ca ions, Journal of Colloids and interface science, 33 (3), 471-472 (1970).

[77] Liu L., Moreno L. Neretnieks I., A Novel Approach to Determine the Critical Coagulation Concentration of a Colloidal Dispersion with Plate-like Particles, Langmuir, 25, 688-697 (2009)

[78] Horikawa Y., Murray R.S., Quirk J.P., The effect of electrolyte concentration on the zetapotential of homoionic montmorillonite and illite, Colloid and Surface 32, 181-195 (1988).

[79] Missana T., Adell A. On the applicability of DLVO theory to the prediction of clay colloid stability. Journal of Colloids and Interface Science, 230(1), 150-156 DOI: 10.1006/jcis.2000.7003 (2000).

[80] Lebron I. and D.L. Suarez, Electrophoretic mobility of illite and micaceous soil clays, Soil Sci. Soc. Am. J, 56 1106-1115 (1992).

[81] Bradbury, M.H., and B. Baeyens. Experimental and modelling studies on the pH buffering of MX-80 bentonite porewater. Applied Geochemistry 24:419-425 (2009).

[82] Fernández, A.M., B. Baeyens, M. Bradbury, and P. Rivas. Analysis of porewater chemical composition of a Spanish compacted bentonite used in engineered barrier. Physics and Chemistry of the Earth 29:105-118 (2004).

[83] Wersin, P., M. Kiczka, and K. Koskinen. 2016. Porewater chemistry in compacted bentonite: Application to the engineered buffer barrier at the Olkiluoto site. Apllied Geochemistry 74:165-175.

[84] Alonso U, Missana T, García-Gutiérrez M, 2007. Experimental approach to study the colloid generation from the bentonite barrier to quantify the source term and to assess its relevance on the radionuclide migration. MRS Online Proceedings Library 985: Scientific Basis for Nuclear Waste Management XXX, 605–610 (2007).

[85] Birgersson, M., L. Börgesson, M. Hedström, O. Karnland, and U. Nilsson. 2009. Bentonite erosion. SKB technical report, TR 09-34, (2009).

[86] Grissinger, E.H. Resistance of selected clay systems to erosion by water. Water Resources Research 2:131-138 (1966).

[87] Banin, A., and N. Lahav. Particle size and optical properties of montmorillonite in suspension. Israel Journal of Chemistry 6:235-250 (1968).

[88] Bell, J.C.L., and P. Stenius. 1980. The Influence of Cations on Particle Interactions and Particle Release from Aqueous Bentonite Gels. Powder Technology 26:17-27 (1980).

[89] Norrish, K. The swelling of montmorillonite. Discussions of the Faraday Society 18:120-134 (1954).

[90] Mantovani, M., A. Escudero, M.D. Alba, and A.I. Becerro. Stability of phyllosilicates in Ca(OH)(2) solution: Influence of layer nature, octahedral occupation, presence of tetrahedral Al and degree of crystallinity. Applied Geochemistry 24:1251-1260 (2009).

[91] Milodowski, A.E., S. Norris, and W.R. Alexander. Minimal alteration of montmorillonite following long-term interaction with natural alkaline groundwater: Implications for geological disposal of radioactive waste. Applied Geochemistry 66:184-197 (2016).

[92] Montes-H, G., B. Fritz, A. Clement, and N. Michau. A simplified method to evaluate the swelling capacity evolution of a bentonite barrier related to geochemical transformations. Applied Geochemistry 20:409-422 (2005).

[93] Goldberg, S., and R.A. Glaubig. Effect of saturating cation, pH and aluminium and iron oxide on the flocculation of kaolinite and montmorillionite. Clays and Clay Minerals 35:220-227 (1987).

[94] Kretzschmar R., Borkovec M., Grolimund D., Elimelech M, Mobile subsurface colloids and their role in contaminant transport, Adv. Agronomy 66, 121–193 (1999).

[95] Tang X., Weisbrod N., Colloid-facilitated transport of lead in natural discrete fractures, Environ. Pollut. 157, 2266–2274 (2009).

[96] Wang D., Paradelo M., Bradford S.A.,. Peijnenburg W.J.G.M, Chu L., Zhou D., Facilitated transport of Cu with hydroxyapatite nanoparticles in saturated sand: effects of solution ionic strength and composition, Water Res. 45 5905–5915 (2011).

[97] Schäfer T, Huber F., Seher H., Missana T., Alonso U., Kumke M., Eidner S., Claret F., Enzmann F., Nanoparticles and their influence on radionuclide mobility in deep geological formations, Appl. Geochem. 27 390–403 (2012).

[98] Honeyman B.D., The role of colloids in radionuclide retention by and transport through geological media, in: Workshop Proceedings on Radionuclide Retention in Geological Media, OECD Publishing Oskarshamn, Sweden, 2001, pp. 91–99 (2001).

[99] Missana T., Alonso U., García-Gutiérrez M., Mingarro M., Role of colloids on the migration of europium and plutonium in a granite fracture, Appl. Geochem. 23, 1484–1497(2008).

[100] Albarran N., Missana T., Garcia-Gutierrez M., Alonso U., Mingarro M., Strontium migration in a crystalline medium: effects ofthe presence of bentonite colloids, J. Contam. Hydrol. 122 (2011) 76–85. (2011) 76–85

[101] Schäfer T., Geckeis H., Bouby M., Fanghänel T.U., Th, Eu and colloid mobility in a granite fracture under near-natural flow conditions, Radiochim. Acta 92 731–737 (2004).

[102] Lahtinen M., Hölttä P., Riekkola M.L., Yohannes G., Analysis of colloids released from bentonite and crushed rock, Phys. Chem. Earth 35, 265–270(2010).

[103] Möri A., Alexander W.R., Geckeis H., Hauser W., Schäfer T., Eikenberg J., Fierz Th., Degueldre C., Missana T., The colloid and radionuclide retardation experiment at the Grimsel Test Site: influence of bentonite colloids on the radionuclide migration in a fractured rock, Colloids Surf. A 217 (1–3) 33–47 (2003).

[104] Pusch R. Clay colloid formation and release from MX-80 buffer, SKB Technical Report TR-99-31 (1999)

[105] Bradford S.A., Yates S.R., Bettahar M., Simunek J., Physical factors affecting the transport and fate of colloids in saturated porous media, Water Resources research Vol 38 (12) 1327 doi:10.1029/2002WR001340 (2002).

[106] Zvikelsky O., Weisbrod N., Impact of particle size on colloid transportin discrete fracture, Water Resour. Res. 42 (W12S08) 12(2006).

[107] Albarran N., Missana T., Alonso U., García-Gutiérrez M., López T. Analysis of latex, gold and smectite colloid transport and retention in artificial fractures in crystalline rocks, Colloids and Surfaces A: Physicochemical and Engineering Aspects 435, 115-126 DOI: 10.1016/j.colsurfa.2013.02.002 (2013).

[108] Wallis, I., A. Idiart, R. Dohrmann, and V. Post. Reactive transport modelling of groundwater-bentonite interaction: Effects on exchangeable cations in an alternative buffer material in-situ test. Applied Geochemistry 73:59-69 (2016).

[109] Fernández, A.M., and M.V. Villar. Geochemical behaviour of a bentonite barrier in the laboratory after up to 8 years of heating and hydration. Applied Geochemistry 25:809-824 (2010).


2695-8864